Fluorescence-based measurements of phosphatidylserine/phosphatidylinositol 4-phosphate exchange between membranes

--Manuscript Draft--

Article Type:	Invited Methods Collection - JoVE Produced Video
Manuscript Number:	JoVE62177R2
Full Title:	Fluorescence-based measurements of phosphatidylserine/phosphatidylinositol 4-phosphate exchange between membranes
Corresponding Author:	Guillaume Drin Centre National de la Recherche Scientifique Sophia-Antipolis, 06560 FRANCE
Corresponding Author's Institution:	Centre National de la Recherche Scientifique
Corresponding Author E-Mail:	drin@ipmc.cnrs.fr
Order of Authors:	Guillaume Drin
	Souade Ikhlef
	Nicolas-Frédéric Lipp
	Maud Magdeleine
Additional Information:	
Question	**Response**
Please specify the section of the submitted manuscript.	Biochemistry
Please indicate whether this article will be Standard Access or Open Access.	Standard Access (US$2,400)
Please indicate the **city, state/province, and country** where this article will be **filmed**. Please do not use abbreviations.	Sophia-Antipolis, 06560, FRANCE
Please confirm that you have read and agree to the terms and conditions of the author license agreement that applies below:	I agree to the Author License Agreement
Please provide any comments to the journal here.	We'd like to integrate if possible the section 3 (liposome preparation) in the movie

1   **TITLE:**
2   Fluorescence-based Measurements of Phosphatidylserine/Phosphatidylinositol 4-Phosphate
3   Exchange Between Membranes
4
5   **AUTHORS AND AFFILIATIONS:**
6   Souade Ikhlef*, Nicolas-Frédéric Lipp*, Maud Magdeleine, Guillaume Drin
7
8   Université Côte d'Azur, Centre National de la Recherche Scientifique, Institut de Pharmacologie
9   Moléculaire et Cellulaire, 660 route des lucioles, 06560 Valbonne, France
10
11 *Equal contribution
12
13 **Email addresses of co-authors:**
14 Souade Ikhlef   ikhlef@ipmc.cnrs.fr
15 Nicolas-Frédéric Lipp   lipp@ipmc.cnrs.fr
16 Maud Magdeleine   magdeleine@ipmc.cnrs.fr
17
18 **Corresponding author:**
19 Guillaume Drin   drin@ipmc.cnrs.fr
20
21 **KEYWORDS:** (Instructions)
22 lipid transfer protein, OSBP-related protein, phosphatidylserine, phosphatidylinositol 4-
23 phosphate, fluorescence, recombinant protein, liposome
24
25 **SUMMARY:**
26 Here, we describe protocols using fluorescent lipid sensors and liposomes to determine whether
27 a protein extracts and transports phosphatidylserine or phosphatidylinositol 4-phosphate *in*
28 *vitro*.
29
30 **ABSTRACT:**
31 Several members of the evolutionarily conserved oxysterol-binding protein (OSBP)-related
32 proteins(ORP)/OSBP homologs (Osh) family have recently been found to represent a novel lipid
33 transfer protein (LTP) group in yeast and human cells. They transfer phosphatidylserine (PS) from
34 the endoplasmic reticulum (ER) to the plasma membrane (PM) *via* PS/phosphatidylinositol 4-
35 phosphate (PI(4)P) exchange cycles. This finding allows a better understanding of how PS, which
36 is critical for signaling processes, is distributed throughout the cell and the investigation of the
37 link between this process and phosphoinositide (PIP) metabolism. The development of new
38 fluorescence-based protocols has been instrumental in the discovery and characterization of this
39 new cellular mechanism *in vitro* at the molecular level. This paper describes the production and
40 the use of two fluorescently labelled lipid sensors, NBD-C2$_{Lact}$ and NBD-PH$_{FAPP}$, to measure the
41 ability of a protein to extract PS or PI(4)P and to transfer these lipids between artificial
42 membranes. First, the protocol describes how to produce, label, and obtain high-purity samples
43 of these two constructs. Secondly, this paper explains how to use these sensors with a
44 fluorescence microplate reader to determine whether a protein can extract PS or PI(4)P from

45   liposomes, using Osh6p as a case study. Finally, this protocol shows how to accurately measure
46   the kinetics of PS/PI(4)P exchange between liposomes of defined lipid composition and to
47   determine lipid transfer rates by fluorescence resonance energy transfer (FRET) using a standard
48   fluorometer.
49
50   **INTRODUCTION:**
51   The precise distribution of lipids between different membranes and within the membranes of
52   eukaryotic cells[1,2] has profound biological implications. Decrypting how LTPs function is an
53   important issue in cell biology[3-6], and *in vitro* approaches are of great value in addressing this
54   issue[7-11]. Here, an *in vitro*, fluorescence-based strategy is presented that has been instrumental
55   in establishing that several ORP/Osh proteins effect PS/PI(4)P exchange between cell
56   membranes[12] and thereby constitute a new class of LTPs. PS is an anionic glycerophospholipid
57   that represents 2–10% of total membrane lipids in eukaryotic cells[13-16]. It is distributed along a
58   gradient between the ER and the PM, where it represents 5–7% and up to 30% of
59   glycerophospholipids, respectively[17-19]. Moreover, PS is essentially concentrated in the cytosolic
60   leaflet of the PM. This build-up and the uneven partition of PS in the PM are critical for cellular
61   signaling processes[19]. Owing to the negative charge of PS molecules, the cytosolic leaflet of the
62   PM is much more anionic than the cytosolic leaflet of other organelles[1,2,19,20]. This enables the
63   recruitment, *via* electrostatic forces, of signaling proteins such as myristoylated alanine-rich C-
64   kinase substrate (MARCKS)[21], sarcoma (Src)[22], Kirsten-rat sarcoma viral oncogene (K-Ras)[23], and
65   Ras-related C3 botulinum toxin substrate 1 (Rac1)[24] that contain a stretch of positively charged
66   amino acids and a lipidic tail.
67
68   PS is also recognized by conventional protein kinase C in a stereoselective manner *via* a C2
69   domain[25]. However, PS is synthesized in the ER[26], indicating that it must be exported to the PM
70   before it can play its role. It was not known how this was accomplished[19] until the finding that, in
71   yeast, Osh6p and Osh7p transfer PS from the ER to the PM[27]. These LTPs belong to an
72   evolutionarily conserved family in eukaryotes whose founding member is OSBP and that contains
73   proteins (ORPs in human, Osh proteins in yeast) containing an OSBP-related domain (ORD) with
74   a pocket to host a lipid molecule. Osh6p and Osh7p contain only an ORD whose structural
75   features are adapted to specifically bind PS and transfer it between membranes. Nevertheless,
76   how these proteins directionally transferred PS from the ER to the PM was unclear. Osh6p and
77   Osh7p can trap PI(4)P as an alternative lipid ligand[12]. In yeast, PI(4)P is synthesized from
78   phosphatidylinositol (PI) in the Golgi and PMs by PI 4-kinases, Pik1p and Stt4p, respectively. In
79   contrast, there is no PI(4)P in the ER membrane, as this lipid is hydrolyzed to PI by the Sac1p
80   phosphatase. Hence, a PI(4)P gradient exists at both the ER/Golgi and ER/PM interfaces. Osh6p
81   and Osh7p transfer PS from the ER to the PM *via* PS/PI(4)P exchange cycles using the PI(4)P
82   gradient that exists between these two membranes[12].
83
84   Within one cycle, Osh6p extracts PS from the ER, exchanges PS for PI(4)P at the PM and transfers
85   PI(4)P back to the ER to extract another PS molecule. Osh6p/Osh7p interact with Ist2p[28], one of
86   the few proteins that connect and bring the ER membrane and the PM into close proximity with
87   each other to create ER-PM contact sites in yeast[29-31]. In addition, the association of Osh6p with
88   negatively charged membranes becomes weak as soon as the protein extracts one of its lipid

89   ligands due to a conformational change that modifies its electrostatic features[32]. This aids Osh6p
90   by shortening its membrane dwell time, thereby maintaining the efficiency of its lipid transfer
91   activity. Combined with the binding to Ist2p, this mechanism could allow Osh6p/7p to both
92   quickly and accurately execute lipid exchange at the ER/PM interface. In human cells, ORP5 and
93   ORP8 proteins execute PS/PI(4)P exchange at ER-PM contact sites *via* distinct mechanisms[33].
94   They have a central ORD, akin to Osh6p, but are directly anchored to the ER *via* a C-terminal
95   transmembrane segment[33] and dock into the PM *via* an N-terminal Pleckstrin homology (PH)
96   domain that recognizes PI(4)P and PI(4,5)P_2[33-35]. ORP5/8 use PI(4)P to transfer PS, and it has been
97   shown that ORP5/8 additionally regulate PM PI(4,5)P_2 levels and presumably modulate signaling
98   pathways. In turn, a decrease in PI(4)P and PI(4,5)P_2 levels suppresses ORP5/ORP8 expression as
99   these proteins associate with the PM in a PIP-dependent fashion. Abnormally high PS synthesis,
100   which leads to Lenz-Majewski syndrome, impacts PI(4)P levels through ORP5/8[36]. When the
101   activity of both proteins is blocked, PS becomes less abundant at the PM, lowering the oncogenic
102   capability of signaling proteins[37].
103
104   Conversely, ORP5 overexpression seems to promote cancer cell invasion and metastatic
105   processes[38]. Thus, alterations to ORP5/8 activity can severely modify cellular behavior through
106   changes in lipid homeostasis. Further, ORP5 and ORP8 occupy ER-mitochondria contact sites and
107   preserve some mitochondrial functions, possibly by supplying PS[39]. Additionally, ORP5 localizes
108   to ER-lipid droplet contact sites to deliver PS to lipid droplets by PS/PI(4)P exchange[40]. The
109   strategy described herein to measure (i) PS and PI(4)P extraction from liposomes and (ii) PS and
110   PI(4)P transport between liposomes has been devised to establish and analyze the PS/PI(4)P
111   exchange activity of Osh6p/Osh7p[12,32] and used by other groups to analyze the activity of
112   ORP5/ORP8[35] and other LTPs[10,41]. It is based on the use of a fluorescence plate reader, a standard
113   L-format spectrofluorometer, and two fluorescent sensors, NBD-C2$_{Lact}$ and NBD-PH$_{FAPP}$, that can
114   detect PS and PI(4)P, respectively. NBD-C2$_{Lact}$ corresponds to the C2 domain of the glycoprotein,
115   lactadherin, that was reengineered to include a unique solvent-exposed cysteine near the
116   presumed PS binding site; a polarity-sensitive NBD (7-nitrobenz-2-oxa-1,3-diazol) fluorophore is
117   covalently linked to this residue (**Figure 1A**)[12].
118
119   The C2 domain of lactadherin (*Bos taurus*, UniProt: Q95114, residues 270–427) was cloned into
120   a pGEX-4T3 vector to be expressed in fusion with glutathione S-transferase (GST). The C2$_{Lact}$
121   sequence was then mutated to substitute two solvent-accessible cysteine residues (C270, C427)
122   with alanine residues and to introduce a cysteine residue into a region near the putative PS-
123   binding site (H352C mutation)[12]. A cleavage site for thrombin is present between the GST protein
124   and the N-terminus of the C2 domain. A major advantage is that this domain selectively
125   recognizes PS in a Ca^{2+}-independent manner contrary to other known C2 domains or Annexin
126   A5[42]. NBD-PH$_{FAPP}$ is derived from the PH domain of the human PI(4)P adapter protein, four-
127   phosphate-adaptor protein 1 (FAPP1), which was reengineered to include a single solvent-
128   exposed cysteine that can be labeled with an NBD group near the PI(4)P binding site (**Figure 1A**)[43].
129   The nucleotide sequence of the PH domain of the human FAPP protein (UniProt: Q9HB20,
130   segment [1-100]) has been cloned into a pGEX-4T3 vector to be expressed in tandem with a GST
131   tag in *Escherichia coli*. The PH$_{FAPP}$ sequence has been modified to insert a unique cysteine residue
132   within the membrane-binding interface of the protein that can be subsequently labeled with

133 *N*,*N*'-dimethyl-*N*-(iodoacetyl)-*N*'-(7-nitrobenz-2-oxa-1,3-diazol-4-yl)   ethylene
134 diamine (IANBD)[43]. Moreover, a nine-residue linker has been introduced between the thrombin
135 cleavage site and the N-terminus of the PH domain to ensure accessibility to the protease.
136
137 To measure PS extraction from liposomes, NBD-C2$_{Lact}$ is mixed with liposomes made of
138 phosphatidylcholine (PC) containing trace amounts of PS. Owing to its affinity for PS, this
139 construct binds to the liposomes, and the NBD fluorophore experiences a change in polarity as it
140 comes into contact with the hydrophobic environment of the membrane, which elicits a blue-
141 shift and an increase in fluorescence. If PS is extracted almost completely by a stoichiometric
142 amount of LTP, the probe does not associate with liposomes, and the NBD signal is lower (**Figure**
143 **1B**)[32]. This difference in signal is used to determine whether an LTP (*e.g.,* Osh6p) extracts PS. A
144 similar strategy is used with NBD-PH$_{FAPP}$ to measure PI(4)P extraction (**Figure 1B**), as described
145 previously[12,32]. Two FRET-based assays were designed to (i) measure PS transport from L$_A$ to L$_B$
146 liposomes, which mimic the ER membrane and the PM, respectively, and (ii) PI(4)P transport in
147 the reverse direction. These assays are performed under the same conditions (*i.e.,* same buffer,
148 temperature, and lipid concentration) to measure PS/PI(4)P exchange**.** To measure PS transport,
149 NBD-C2$_{Lact}$ is mixed with L$_A$ liposomes composed of PC and doped with 5 mol% PS and 2 mol% of
150 a fluorescent lipid—rhodamine-phycoerythrin (Rhod-PE)—and L$_B$ liposomes incorporating 5
151 mol% PI(4)P.
152
153 At time zero, FRET with Rhod-PE quenches the NBD fluorescence. If PS is transported from L$_A$ to
154 L$_B$ liposomes (*e.g.,* upon injecting Osh6p), a fast dequenching occurs due to the translocation of
155 NBD-C2$_{Lact}$ molecules from L$_A$ to L$_B$ liposomes **(Figure 1C)**. Given the amount of accessible PS,
156 NBD-C2$_{Lact}$ remains essentially in a membrane-bound state over the course of the experiment[12].
157 Thus, the intensity of the NBD signal directly correlates with the distribution of NBD-C2$_{Lact}$
158 between L$_A$ and L$_B$ liposomes and can be easily normalized to determine how much PS is
159 transferred. To measure the transfer of PI(4)P in the opposite direction, NBD-PH$_{FAPP}$ is mixed with
160 L$_A$ and L$_B$ liposomes; given that it only binds to L$_B$ liposomes that contain PI(4)P, but not Rhod-PE,
161 its fluorescence is high. If PI(4)P is transferred to L$_A$ liposomes, it translocates to these liposomes,
162 and the signal decreases due to FRET with Rhod-PE **(Figure 1C)**. The signal is normalized to
163 determine how much PI(4)P is transferred[43].
164
165 **PROTOCOL:**
166
167 **1. Purification of NBD-C2$_{Lact}$**
168
169 NOTE: Although this protocol details the use of a cell disruptor to break bacteria, it can be
170 modified to use other lysis strategies (*e.g.,* a French press). At the beginning of the purification,
171 it is mandatory to use buffer that is freshly degassed, filtered, and supplemented with 2 mM
172 dithiothreitol (DTT) to prevent the oxidation of cysteine. However, for the protein labelling step,
173 it is crucial to completely remove DTT. Many steps must be carried out on ice or in a cold room
174 to avoid any protein degradation. Samples of 30 µL volume must be collected at different steps
175 of the protocol to perform an analysis on a 15% acrylamide sodium dodecylsulfate-
176 polyacrylamide gel electrophoresis (SDS-PAGE) gel to check the progress of the purification. Mix

177 enough denaturing Laemmli sample buffer with each aliquot, and heat the mixture at 95 °C.
178 Freeze and store the tubes at -20 °C until analysis.
179
180 1.1   Expression of GST-C2$_{Lact}$ in *Escherichia coli*
181
182 1.1.1. Mix 20 µL of BL21 Gold competent cells with 18 µL of sterilized water. Then, mix 2 µL of
183 pGEX-C2$_{Lact}$ plasmid (at ~65 ng/µL) with the bacteria, and transform them by electroporation.
184 Resuspend the bacteria with 150 µL of autoclaved Lennox Luria-Bertani (LB) broth medium (10
185 g/L tryptone, 5 g/L yeast extract, 5 g/L NaCl in deionized water, glucose-free). Let the bacteria
186 grow at 37 °C for 1 h in a 2 mL snap-cap microcentrifuge tube.
187
188 1.1.2. Inoculate 25 mL of LB medium, supplemented with 50 µg/mL ampicillin, with 150 µL of
189 bacterial suspension in a 125 mL sterile Erlenmeyer flask. Place the flask in an orbital shaker at
190 37 °C, and let the bacteria grow overnight with agitation at 185 rpm.
191
192 1.1.3. Fill two sterile 2 L Erlenmeyer flasks with 500 mL of LB medium supplemented with 50
193 µg/mL ampicillin, and add 5 mL of preculture suspension. Let the bacteria grow at 37 °C with
194 agitation at 220 rpm.
195
196 1.1.4. Periodically measure the optical density (OD) of the suspension at a wavelength (λ) of 600
197 nm. When the OD reaches a value of ~0.6–0.7, add 500 µL of a stock solution of 1 M isopropyl β-
198 D-1-thiogalactopyranoside (IPTG) to each flask to initiate the expression of GST-C2$_{Lact}$. Shake the
199 flasks at 185 rpm for 4 h at 37 °C.
200
201 1.1.5. Transfer the contents of each flask to a polypropylene centrifuge bottle. Centrifuge the
202 two bottles for 30 min at 3000 × *g* at 4 °C to pellet the bacteria. Discard the supernatant, and
203 resuspend each pellet in 50 mL of cold phosphate-buffered saline.
204
205 1.1.6. Transfer the bacterial suspension contained in each bottle to a 50 mL conical centrifuge
206 tube. Centrifuge the two tubes for 30 min at 3500 × *g* at 4 °C. Remove the supernatant, and store
207 the tubes, each of which contains a bacterial pellet, at -20 °C.
208
209 1.2.   Purification of C2$_{Lact}$
210
211 1.2.1. On ice, fill two 50 mL conical centrifugal tubes with 50 mL of buffer containing 50 mM
212 Tris-HCl, pH 7.4, and 150 mM NaCl (hereafter called TN buffer), previously filtered and degassed
213 by membrane vacuum filtration.
214
215 1.2.2. To prepare the lysis buffer in each tube, add dissolve an ethylenediamine tetraacetic acid-
216 free protease inhibitor cocktail in the TN buffer by mild sonication or vortexing. Add other
217 antiproteases, (10 µM bestatin, 1 µg/mL pepstatin A, and 10 µM mM phosphoramidon).
218 Importantly, supplement the buffer with 2 mM DTT.
219
220 1.2.3. Fill the two tubes that contain the bacterial pellets prepared in step 1.1.6, with lysis buffer

221 to obtain a final volume of 30 mL in each tube, and slowly defrost the pellets on ice for 10 min.
222 Crush each pellet with a stainless steel spatula, and resuspend them by vortexing the tubes
223 and/or by pipetting the suspension back and forth with a pipette controller and a 25 mL pipette
224 until a homogeneous suspension is obtained.
225
226 1.2.4.   Perform lysis using a precooled cell disruptor (see the **Table of Materials**) by loading 30
227 mL of the sample inside the reservoir and running a breaking cycle in continuous mode with a
228 pressure of 1.6 bar. Collect the lysate in the same tube, keep the tube on ice, and immediately
229 add 250 μL from a stock solution of 200 mM phenylmethylsulfonyl fluoride (PMSF) prepared in
230 isopropanol.
231
232 1.2.5.   Lyse the other sample following the same procedure. Use the remainder of the lysis buffer
233 to wash the cell disruptor, and collect the wash to adjust the volume of each lysate (~30 mL) to a
234 final volume of 50 mL.
235
236 1.2.6.   Supplement each lysate with 5 mM $MgCl_2$, and add 5 μg/mL of DNAse I to fragment the
237 DNA and thus reduce the viscosity of the sample. Incubate on ice for 30 min. Collect a sample for
238 gel analysis.
239
240 1.2.7.   Transfer each 50 mL lysate to a prechilled polycarbonate ultracentrifuge tube (two in
241 total, see the **Table of Materials**). Centrifuge at 186,000 × g at 4 °C for at least 1 h using an
242 ultracentrifuge.
243
244 1.2.8.   In parallel to the centrifugation step, dispense 1.4 mL of a slurry containing glutathione
245 coupled to 4% agarose into two 50 mL conical centrifugal tubes, add 20 mL of TN buffer
246 supplemented with 1 mM DTT (TND buffer) to each tube, centrifuge at 500 × g for 5 min, and
247 discard the supernatant. Repeat this washing step twice.
248
249 1.2.9.   After the centrifugation of the bacterial lysate, remove a 30 μL sample from the
250 supernatant, and transfer the supernatant from each ultracentrifuge tube to a corresponding 50
251 mL conical centrifuge tube that contains clean beads. For gel analysis, resuspend the debris pellet
252 in one of the ultracentrifuge tubes with 50 mL of TND buffer, and collect a 30 μL sample.
253
254 1.2.10. Place the tubes on a rotator for 3–4 h at 4 °C to obtain a homogeneous bead suspension.
255 Pool the bead suspensions in an empty 25 mL chromatography column. Let the beads decant,
256 and remove the buffer and unbound proteins by gravity flow. Take a sample from the eluate for
257 analysis.
258
259 1.2.11. Resuspend the beads with 20 mL of TND buffer, and collect the eluate by gravity flow.
260 Repeat this step twice to completely wash the beads. Pool the collected eluates, and retain a 30
261 μL sample for further analysis.
262
263 NOTE: After a short decantation, a volume of ~2 mL of bead suspension, to which GST-C2$_{Lact}$ is
264 attached, sediments at the bottom of the column.

265

266   1.2.12. Add 1 mL of bead suspension to two 2 mL snap-cap microcentrifuge tubes. Fill each tube
267   with TND buffer to a final volume of 1.970 mL. Take a 30 µL sample from one tube for further
268   analysis (B1 sample). Add 10 µL of 10 mM $CaCl_2$ solution and 25 µL from a stock solution of human
269   thrombin protease solution at 0.02 U/µL.

270

271   1.2.13. Place the two tubes on a rotator at 4 °C overnight to allow thrombin to cleave off the GST
272   tag from the $C2_{Lact}$ domain. On the next day, in each tube, mix 10 µL of 200 mM PMSF solution
273   with the bead suspension to inhibit the thrombin action.

274

275   1.2.14. Centrifuge the tubes at 700 × g for 5 min, and collect the supernatant, which contains
276   soluble $C2_{Lact}$ domain, from each tube, without taking the beads. Pool the supernatants into a 2
277   mL snap-cap microcentrifuge tube (E1 eluate) that is kept on ice.

278

279   1.2.15. Add 1 mL of TN buffer to each tube to resuspend the beads, and wash them; repeat step
280   1.2.14. Perform this step thrice more to recover a maximum amount of protein. Each time, pool
281   the collected supernatants into a new 2 mL tube (E2, E3, E4, and E5 eluates), and take an aliquot
282   for further analysis. At the end of washing steps, take an aliquot from the bead suspension
283   (aliquot B2).

284

285   1.2.16. Analyze the 30 µL samples that were collected at the different steps of the purification
286   protocol by SDS-PAGE separation on a 15% acrylamide gel.

287

288   1.2.17. Remove potential contaminating beads by pooling all the supernatants (*i.e.*, ~10 mL)
289   collected during steps 1.2.14 and 1.2.15 into a 10 mL chromatography column. Collect the eluate
290   by gravity flow, and retain the beads at the bottom of the column.

291

292   1.2.18. Concentrate the $C2_{Lact}$ sample using a centrifugal filter unit with a molecular weight cut-
293   off (MWCO) of 3 kDa and a centrifugation speed of 1500 × g. Stop the concentration procedure
294   when the volume of the protein sample is ~1 mL.

295

296   1.3.   Preparation and purification of NBD-$C2_{Lact}$

297

298   1.3.1. Equilibrate a desalting column (see the **Table of Materials**) with TN buffer. Load the
299   column with 1 mL of concentrated $C2_{Lact}$ sample. Allow the sample to enter the gel bed
300   completely, add 1.5 mL of freshly degassed DTT-free TN buffer to the column, and collect the
301   eluate by gravity flow into a 2 mL snap-cap microcentrifuge tube.

302

303   1.3.2. Dilute 50 µL of eluate in a final volume of 300 µL TN buffer, and record an absorbance
304   spectrum from 230 to 450 nm using pure TN buffer as a blank. Determine the $C2_{Lact}$ concentration
305   based on the absorbance measured at 280 nm, considering an extinction coefficient ε equal to
306   44,920 $M^{-1}.cm^{-1}$.

307

308   1.3.3. To label the $C2_{Lact}$ construct with a NBD fluorophore, mix the protein with a ten-fold molar

309 excess of *N,N'*-dimethyl-*N*-(iodoacetyl)-*N'*-(7-nitrobenz-2-oxa-1,3-diazol-4-yl)ethylenediamine
310 (IANBD amide).
311
312 1.3.3.1.   Dissolve 1 mg of IANBD in anhydrous dimethylformamide (DMF), keeping in mind
313 that the final volume of DMF used for labeling the $C2_{Lact}$ construct must not exceed 5% (v/v) of
314 the protein sample volume.
315
316 1.3.3.2.   To determine the volume of DMF (V_{DMF}) to dissolve IANBD, first calculate the
317 required amount of IANBD (m, expressed in mg) to label the protein by using formula **1**.
318
319 $m = 10{,}000 \times C \times V \times MW_{IANBD}$ (**1**)
320
321 where C is the concentration of $C2_{Lact}$ measured in step 1.3.2, V is the volume of the $C2_{Lact}$ sample,
322 and MW_{IANBD} is the molecular weight of the fluorophore (420 g/mol).
323
324 1.3.3.3.   Calculate V_{DMF} by using formulae **2** (with $m_0=1$) and **3**.
325
326 $V_{DMF}= (m_0/m) \times V_{IANBD}$ (**2**)
327
328 $V_{IANBD}=0.05 \times V$ (**3**)
329
330 Where m_0 is the quantity of IANBD powder in mg, and V_{IANBD} is the volume of IANBD solution to
331 be added to the $C2_{Lact}$ sample.
332
333 1.3.3.4.   Add volume V_{IANBD} of the freshly-prepared IANBD solution to the $C2_{Lact}$ sample,
334 and shake the reaction mixture at 800–900 rpm for 30 min at 25 °C using a thermomixer
335 protected from light. Let the reaction proceed for 90 min on ice. In the meantime, clean a
336 centrifugal filter unit (MWCO= 3 kDa) with 10 mL of TN buffer.
337
338 1.3.4. Add L-cysteine in (10-fold molar excess to IANBD) to the reaction mixture to inactivate
339 free IANBD. Add 15 mL of TN buffer to the NBD-$C2_{Lact}$ solution, and transfer the NBD-$C2_{Lact}$
340 solution to the centrifugal filter unit.
341
342 1.3.5. Concentrate the sample to 2 mL to separate most of the free NBD from the protein by
343 centrifugation at 1500 × *g*. Repeat this washing step two times. Centrifuge the sample in a 2 mL
344 snap-cap centrifuge tube for 10 min at 25,000 × *g* at 4 °C to pellet potential aggregates, and
345 collect the supernatant.
346
347 1.3.6. Dilute 50 µL of eluate in a final volume of 300 µL of TN buffer. Record the absorbance
348 spectrum from 230 to 650 nm using the eluate collected during the concentration procedure as
349 a blank. Determine the NBD-$C2_{Lact}$ concentration using the maximal absorbance at λ=280 and 495
350 nm and extinction coefficients ε= 44,920 $M^{-1}.cm^{-1}$ (protein) and 25,000 $M^{-1}.cm^{-1}$ (NBD
351 fluorophore).
352

353 NOTE: If the two concentration values are alike, this indicates that the C2$_{Lact}$ construct is labeled
354 at a 1:1 ratio with the NBD group.
355
356 1.3.7. If the NBD-C2$_{Lact}$ concentration estimated from the measurement of NBD absorbance
357 exceeds the concentration estimated from the absorbance of tryptophan (Trp) residues, repeat
358 step 1.3.4 to further remove free NBD.
359
360 1.3.8. Add glycerol to the sample to obtain a final concentration of 10% (v/v) to cryo-protect the
361 NBD-C2$_{Lact}$ construct during flash-freezing. Measure the final protein concentration.
362
363 1.3.9. Prepare 50 µL aliquots of protein in 0.5 mL snap-cap microcentrifuge tubes. Flash-freeze
364 the tubes in liquid nitrogen, and store them at -80 °C.
365
366 **2.   Purification of NBD-PH$_{FAPP}$**
367
368 NOTE: The procedure to produce and label PH$_{FAPP}$ is identical to that of NBD-C2$_{Lact}$ until the
369 transfer of NBD-C2$_{Lact}$ solution to a centrifugal filter unit in step 1.3.4. From this step onwards,
370 follow the protocol that is described below.
371
372 2.1.   After the concentration step, keep 2 mL of NBD-PH$_{FAPP}$ at 4 °C in the dark for not more
373 than 1 day before performing size-exclusion chromatography. Prior to size-exclusion
374 chromatography, verify that there is no orange deposit (aggregation during concentration) at the
375 bottom of the tube. If this is the case, centrifuge the sample at 540,000 × g for 10 min at 4 °C,
376 and purify the supernatant by size-exclusion chromatography.
377
378 NOTE: Size-exclusion chromatography is performed on a column packed with crosslinked
379 dextran-acrylamide copolymer (see the **Table of Materials**), previously equilibrated with TND
380 buffer, using a fast protein liquid chromatography system (see the **Table of Materials**). The
381 column must be protected from light. A flow rate of 1 mL/min was used, and the elution of the
382 NBD-PH$_{FAPP}$ construct was followed by recording the absorbance at λ=280 (protein) and 480 nm
383 (NBD) at the column exit.
384
385 2.1.1. Inject the NBD-PH$_{FAPP}$ sample loaded in a 2 mL injection loop onto the column, and
386 immediately collect 2.5 mL fractions of eluate.
387
388 2.2.   Analyze all the fractions that correspond to the main peak detected at 280 and 480 nm
389 on a 15% SDS-PAGE gel. Mix a 25 µL sample of each fraction with 15 µL of Laemmli sample buffer
390 prior to heating and loading onto the gel.
391
392 NOTE: A main peak, which is simultaneously detected at λ= 280 and 480 nm, appears once a
393 volume of ~150 mL buffer is passed through the column.
394
395 2.3.   Pool the fractions that exclusively contain NBD-PH$_{FAPP}$ protein (~12.2 kDa), and add
396 glycerol at a final concentration of 10% (v/v). Concentrate the sample using a centrifugal filter

397   unit with a MWCO of 3 kDa to a final volume of 1 mL using a centrifugation speed of 1500 × *g*.
398

399   2.4.   Prepare aliquots, and record an absorbance spectrum as described for NBD-C2$_{Lact}$. Use an
400   extinction coefficient ε= 29,450 M^{-1}.cm^{-1} to determine the concentration of the protein based on
401   the absorbance measured at λ=280 nm.
402

403   **3.**   **Preparation of liposomes for PS and PI(4)P extraction or transfer assays**
404

405   NOTE: Perform all the steps at room temperature unless otherwise specified. Handle organic
406   solvents, rotavapor, and liquid nitrogen with caution.
407

408   3.1.   Prepare   fresh,   filtered,   and   degassed   50   mM   4-(2-hydroxyethyl)-1-
409   piperazineethanesulfonic acid (HEPES)-potassium hydroxide (KOH), pH 7.4, 120 mM potassium
410   acetate (HK) buffer.
411

412   3.2.   For each type of liposome, take precise amounts of different lipids from stock solutions,
413   and mix them in a 25 mL pear-shaped glass flask (**Table 1**). Add pure chloroform to adjust the
414   volume of each mixture to 1 mL. Label each flask with the liposome name. Wrap the flasks
415   containing lipid mixture doped with Rhod-PE with aluminum foil.
416

417   3.3.   Place the flask on a rotary evaporator. Dry the lipids under vacuum and at 25 °C for at
418   least 30 min at a rotation speed of 500 rpm. For lipid films that contain PI(4)P, prewarm the flask
419   at 32–34 °C for 5 min, under gentle rotation, to properly mix PI(4)P with the other lipids before
420   creating vacuum in the flask to remove the solvent, which will leave behind a film of dry lipids on
421   the flask wall.
422

423   3.4.   Disconnect the flask from the evaporator, and place it in a vacuum chamber for 45 min to
424   remove any remaining traces of solvent. Fill the flask with 2 mL of HK buffer, and add a few 4
425   mm-diameter glass beads to the solution. Gently vortex the flask for 2 min to resuspend the lipids
426   and prepare multilamellar lipid vesicles (MLVs) with a lipid concentration of 4 mM. Prepare 0.5
427   mL aliquots of MLVs in 1.5 mL screw-cap microcentrifuge tubes.
428

429   3.5.   Freeze-thaw the tubes 5x (using liquid nitrogen and a water bath at 37 °C, respectively).
430   Extrude the liposomes or store them at -20 °C.
431

432   3.5.1.   Use a mini extruder to prepare the liposomes (*i.e.,* large unilamellar vesicles) from the
433   MLVs according to the manufacturer's guidelines. Use a polycarbonate filter with uniform
434   cylindrical pores of 200 nm diameter.
435

436   3.5.2.   To prepare each type of liposome, extrude at least 250 μL of the corresponding
437   suspension of MLVs. Store the extruded liposomes at 4 °C and in the dark if they contain Rhod-
438   PE. Use the liposomes within 2 days.
439

440   [Insert **Table 1** here]

441

4. Measurement of PS or PI(4)P extraction

442

443

NOTE: Measurements must be conducted using a black 96-well plate and a fluorescence plate reader equipped with monochromators: one for fluorescence excitation and one for emission, with a variable bandwidth.

4.1. Prepare fresh, filtered, and degassed HK buffer supplemented with 1 mM $MgCl_2$ (HKM buffer). Prepare pure PC liposomes and PC liposomes doped with 2 mol% PS or 2 mol% PI(4)P (4 mM final lipid concentration, see **Table 1**).

444
445
446

NOTE: Keep the tubes filled with the suspension of extruded liposomes at room temperature throughout the experiment, and keep the proteins on ice. Additionally, protect the lipid sensors from light.

447

4.2. For the PS extraction assay, in one well, mix liposomes containing 2 mol% PS (80 µM final lipid concentration, 0.8 µM accessible PS concentration) with NBD-C2$_{Lact}$ (250 nM final concentration) in a final volume of 100 µL. Fill a second well with the same amount of liposome (80 µM, 2 mol% PS) and NBD-C2$_{Lact}$ (250 nM) mixed with 3 µM LTP (Osh6p as a positive control or a protein of interest).

NOTE: An incubation time of 5 min is sufficient for Osh6p to achieve lipid extraction.

4.3. Fill a third well with NBD-C2$_{Lact}$ (250 nM) mixed with pure PC liposomes (80 µM). Fill a fourth well only with pure PC liposomes (80 µM). Repeat steps 4.1–4.3 to prepare three additional series of four wells.

4.4. For each well, record an NBD spectrum from 505 to 650 nm (bandwidth 5 nm) upon excitation at 490 nm (bandwidth 5 nm) at 25 °C. For each series, subtract the spectrum recorded with only liposomes from the other spectra.

NOTE: F and F_{max} correspond to the intensity at 536 nm measured with PS-containing liposomes in the presence or absence of LTP, respectively, whereas F_0 is the intensity at the same wavelength with pure PC liposomes. For each series, the percentage of accessible PS that is extracted by the protein is given by using the following formula.

$$100 \times (1-((F-F_0)/(F_{max}-F_0))) \qquad \textbf{(4)}$$

4.5. For the PI(4)P extraction assay, prepare liposomes doped with 2 mol% PI(4)P, and carry out measurements with the NBD-PH$_{FAPP}$ probe. Perform control experiments and determine the extraction percentage in the same way as described above.

NOTE: Liposome and protein concentration are identical to those used in the PS extraction assay.

448

5.   Real-time measurement of PS transport

NOTE: A standard fluorimeter (90° format) equipped with a temperature-controlled cell holder and a magnetic stirrer is used to record lipid transfer kinetics. To accurately acquire data, it is key to permanently maintain the sample at the same temperature (set between 25 and 37 °C depending on the origin of the protein (*e.g.*, yeast or human)) and to constantly stir it. The protocol described below is for the measurement of lipid transport in a 600 µL sample contained in a cylindrical quartz cell.

5.1.   Prepare freshly degassed and filtered HKM buffer. Keep the tubes containing extruded liposomes at room temperature. Wrap tubes containing liposomes with Rhod-PE in aluminum foil, and/or store them in an opaque box to prevent any photobleaching.

5.2.   Adjust the excitation and emission monochromators at λ = 460 nm (with a short bandwidth (1-3 nm)) and at λ = 530 nm (with a large bandwidth ($\geq$ 10 nm)), respectively. Set the acquisition time at 25 min with a time resolution $\leq$ 1 s.

5.3.   In the quartz cuvette, dilute 30 µL of the L_A liposome suspension and a volume of NBD-$C2_{Lact}$ stock solution in prewarmed HKM buffer to prepare a 570 µL sample that contains 200 µM total lipids and 250 nM NBD-$C2_{Lact}$. Add a small magnetic stirring bar, and position the cuvette in the fluorometer holder.

5.4.   Once the sample is thermally equilibrated (after 3–5 min), trigger the measurement. After 1 min, add 30 µL of L_B liposome suspension (final concentration of 200 µM total lipids) to the sample. After 3 min, inject LTP into the sample so that the final concentration of the LTP is 200 nM, and acquire the signal for the remaining 21 min.

5.5.   Carry out a parallel experiment to normalize the NBD signal. Mix 30 µL of L_{A-Eq} liposome suspension with 250 nM NBD-$C2_{Lact}$ in HKM buffer (final volume of 570 µL). After 1 min, inject 30 µL of L_{B-Eq} liposome suspension.

NOTE: The lipid composition of L_{A-Eq} and L_{B-eq} liposomes are similar to that of L_A and L_B liposomes used in the transfer assay, except that each of them contains 2.5 mol% PS and 2.5 mol% PI(4)P. As a result, the NBD signal that is measured, referred to as F_{Eq}, corresponds to the signal that should be measured if PS was fully equilibrated between L_A and L_B liposomes by a transfer process.

5.6.   Convert the kinetic curves measured with an LTP of interest to determine the amount of PS (in µM) transferred from L_A to L_B liposomes over time. Normalize each data point (F) of the curve by using the following formula.

$$F_{Norm} = (F-F_0)/(F_{Eq}-F_0) \qquad (5)$$

in which F_0 corresponds to the NBD signal just before the addition of an LTP, and F_{Eq} is the signal

12

measured in step 5.5.

NOTE: The amount of PS (in µM) transferred from L_A to L_B liposomes corresponds to 2.5 × F_{Norm}, considering that the equilibrium corresponds to a situation where one half of accessible PS molecules, contained in the outer leaflet of the L_A liposomes, (*i.e.*, corresponding to 5 mol% of 0.5 × 200 µM total lipids) has been transferred into L_B liposomes.

6.   Real-time measurement of PI(4)P transport

6.1.   Set the fluorimeter (excitation and emission wavelength, bandwidth, acquisition time, time resolution) as done for the PS transfer assay. Likewise, use the same buffer, cuvette, and liposomes to perform the experiments under constant stirring at the same temperature.

6.2.   In the cuvette, mix 30 µL of L_B liposome suspension and NBD-PH$_{FAPP}$ with prewarmed HKM buffer to obtain a final volume of 570 µL (200 µM total lipids, 250 nM NBD- PH$_{FAPP}$). Once the thermal equilibration of the sample is reached, start the measurement, and after 1 min, inject 30 µL of L_A liposome suspension. After 3 min, inject the LTP of interest (final concentration of 200 nM), and record the signal.

6.3.   Perform a second experiment to normalize the NBD signal. Mix 30 µL of L_{B-Eq} liposome suspension with 250 nM NBD-PH$_{FAPP}$ in 570 µL of HKM buffer. After 1 min, inject 30 µL of L_{A-Eq} liposome suspension.

NOTE: Here, the NBD signal, referred to as F_{Eq}, corresponds to the one which should be measured if PI(4)P was fully equilibrated between L_A and L_B liposomes.

6.4.   Convert the kinetic curves to determine the amount of PI(4)P (in µM) transferred from L_B to L_A liposomes over time. Each data point (F) is normalized by using formula **5** in which F_0 corresponds to the NBD signal prior to the addition of an LTP, and F_{Eq} is the signal measured in step 6.3.

NOTE: The amount of PI(4)P (in µM) transferred from L_A to L_B liposomes corresponds to 2.5 × F_{Norm}, considering that the equilibrium corresponds to a situation where one half of the PI(4)P contained in the outer leaflet of the L_B liposomes (*i.e.,* 0.5 × 5 µM) has been transferred in L_A liposomes.

7.   Analysis of kinetics curves

7.1.   Quantify the extent to which an LTP is efficient by determining the speed at which this LTP transfers lipids from one liposome population to the other one in the first few seconds following its injection to the cuvette.

7.1.1.   Perform a linear regression of the first data points of the transfer kinetics to obtain a slope. Divide the slope value by the LTP concentration in the reaction mixture to determine the

REPRESENTATIVE RESULTS

Figure 2A shows an SDS-PAGE analysis of the products of different steps leading to the purification of $C2_{Lact}$. Lane 1 shows the protein profile of the lysed bacteria expressing GST-$C2_{Lact}$ (~44.8 kDa), whereas lanes 2 and 3 respectively show the protein profiles of the supernatant and bacterial debris after ultracentrifugation. The comparison of these lanes shows that GST-$C2_{Lact}$ has been recovered in the supernatant and thus can be isolated using glutathione-linked agarose beads. Lanes 4 and 5 show the protein profiles of the supernatant after incubation with beads and washes recovered by gravity flow, whereas lane 6 shows the profile of proteins that have been retained on the beads. An analysis of these lanes indicates that almost all GST-$C2_{Lact}$ has been recovered from the beads.

Lanes 8–12 show the presence of a major band corresponding to $C2_{Lact}$ (~17.9 kDa) in the supernatants recovered through successive washes of the beads after thrombin treatment. Lane 13 indicates that non-cleaved GST-$C2_{Lact}$, along with GST (~26.9 kDa), remained bound to beads after this treatment. The comparison of these lanes indicates that the cleavage procedure, albeit not 100% efficient, did yield $C2_{Lact}$ that was then fluorescently labelled. **Figure 2B** shows an ultraviolet (UV)-visible absorbance spectrum of $C2_{Lact}$ labelled with NBD. As the construct is 100% pure, these results confirm that all $C2_{Lact}$ molecules were labelled with an NBD group based on the optical density measured at 280 nm (Trp) and 495 nm (NBD). The purity of NBD-$C2_{Lact}$ and its fluorescence were determined by SDS-PAGE analysis (**Figure 2C**).

[Insert Figure 2]

Figure 3 shows the results from PS and PI(4)P extraction assays using Osh6p. When only incubated with liposomes containing 2 mol% PS, the fluorescence of NBD-$C2_{Lact}$ was maximal as the NBD fluorophore was inserted in the membrane (*i.e.,* a hydrophobic context), indicating that the sensor was membrane-bound. In the presence of Osh6p, the fluorescence was lower and comparable to that measured with pure PC liposomes **(Figure 3A)**. The normalization of intensity values at 536 nm indicated that ~75% of accessible PS was extracted. In the second assay, NBD-PH_{FAPP} was mixed with liposomes containing 2 mol% PI(4)P. The NBD signal was high without Osh6p, but low when Osh6p was present and was similar to that measured with PI(4)P-free liposomes (**Figure 3B**). An analysis of the intensity revealed that ~100 % of accessible PI(4)P was extracted by the LTP.

[Insert Figure 3]

Figure 4A shows typical results from a PS transfer assay using Osh6p as an LTP. At time zero, NBD-$C2_{Lact}$ was mixed with L_A liposomes containing 5 mol% 16:0/18:1-PS (POPS) and 2 mol% Rhod-PE in a volume of 570 μL of HKM buffer at 30 °C. As the probe bound to L_A liposomes, its signal was quenched due to FRET with Rhod-PE present in these liposomes. After one minute, Rhod-PE-free L_B liposomes (30 μL) were added; this was expected to only elicit a slight change in the signal due to light diffusion by this second liposome population and/or a dilution effect. The signal intensity after the addition of the L_B liposomes corresponds to F_0. The injection of a few μL of a stock solution

14

581 of Osh6p (typically 40 µM) to dilute 200 nM of the protein in the reaction mix elicited a slow
582 increase in the NBD signal due to the dequenching of the fluorophore as PS was transported from
583 L_A to L_B liposomes, thereby promoting the translocation of NBD-C2$_{Lact}$.

585 When L_B liposomes contained 5 mol% PI(4)P, the dequenching was much faster, as PS was
586 transferred more rapidly by Osh6p to L_B liposomes due to the counterexchange of PS with PI(4)P
587 by the LTP (second curve). The third curve corresponds to an experiment in which NBD-C2$_{Lact}$ was
588 mixed with equal amounts of L_{A-Eq} and L_{B-Eq} liposomes. The signal was higher than F_0 and
589 corresponded to a situation where the probe was evenly bound to L_A and L_B liposomes, thus
590 reflecting a situation where PS was fully equilibrated between the two populations of liposomes.
591 F_{Eq} was calculated by averaging the value of the signal measured in the last 5 min of the experiment.

593 **[Insert Figure 4]**

595 **Figure 4B** shows average kinetic curves of PS transfer from L_A liposomes to L_B liposomes, doped or
596 not doped with PI(4)P after the normalization of F data using F_0 and F_{Eq} as reference values. The
597 initial transport rate for each experiment was calculated by fitting the initial data points measured
598 after the injection of the protein with a linear function. **Figure 4C** shows the mean initial PS
599 transport rate determined from three distinct experiments using L_B liposomes with or without
600 PI(4)P. When L_B liposomes contained 0 and 5 mol% PI(4)P, the rates were respectively equal to 1.4
601 and 15.8 PS.min^{-1} per Osh6p molecule. **Figure 5A** shows typical results from a PI(4)P transfer assay
602 using Osh6p as an LTP, which was carried out with the same materials and conditions as those
603 used for the PS transport assay.

605 **[Insert Figure 5]**

607 At time zero, NBD-PH$_{FAPP}$ was mixed with L_B liposomes containing 5 mol% PI(4)P in a volume of
608 570 µL of HKM buffer. Because NBD-PH$_{FAPP}$ was bound to L_B liposomes, its signal was high. After
609 one minute, L_A liposomes (30 µL) were added, which was expected to only elicit a slight change
610 in the signal. The intensity then corresponded to F_0. Injecting Osh6p (200 nM final concentration)
611 into the reaction mix triggered a quenching of the NBD signal due to the translocation of NBD-
612 PH$_{FAPP}$ molecules to L_A liposomes as PI(4)P was transferred from L_B liposomes to L_A liposomes.
613 When L_A liposomes contained 5 mol% POPS, the dequenching was much faster owing to a faster
614 PI(4)P transfer resulting from PS/PI(4)P exchange. The third curve corresponds to an experiment
615 in which NBD-PH$_{FAPP}$ was mixed with equal amounts of L_{A-Eq} and L_{B-Eq} liposomes.

617 The signal was lower than F_0 as it corresponded to a situation where the probe was uniformly
618 bound to L_A and L_B liposomes, thus indicative of a full equilibration of PI(4)P between the
619 liposomes. F_{Eq} was calculated by averaging the value of the signal measured in the last 5 min of
620 the experiment. **Figure 5B,C** show averaged kinetics curves obtained after signal normalization
621 and mean PI(4)P initial transfer rates measured with L_A liposomes that were doped or not doped
622 with 5 mol% PS. Here, it is worth noting that both lipid ligands were transported faster and with
623 similar velocities when each lipid was initially present in L_A and L_B membranes, respectively, which
624 indicates that Osh6p is a PS/PI(4)P exchanger.

15

625

627 **Figure 1: Description of the fluorescent lipid sensors and *in vitro* assays.** (**A**) Three-dimensional
628 models of NBD-C2$_{Lact}$ and NBD-PH$_{FAPP}$ based on the crystal structure of the C2 domain of bovine
629 lactadherin (PDB ID: 3BN6[48]) and the NMR structure of the PH domain of the human FAPP1
630 protein (PDB ID: 2KCJ[46]). An *N,N'*-dimethyl-*N*-(thioacetyl)-*N'*-(7-nitrobenz-2-oxa-1,3-diazol-4-
631 yl)ethylenediamine moiety, built manually and energetically minimized, was grafted onto the
632 thiol function of C352 (NBD-C2$_{Lact}$) and C13 (NBD-PH$_{FAPP}$) residues (represented as spheres, with
633 carbon in green, nitrogen in blue, oxygen in red, sulfur in yellow, and hydrogen in white). The
634 surface of the lipid-binding site of each probe was colored in blue. (**B**) Extraction assays. In the PS
635 extraction assay, PC/PS liposomes (98/2 mol/mol) were incubated with 250 nM NBD-C2$_{Lact}$. In the
636 absence of extraction, the probe strongly bound to the liposomes, resulting in a blue shift of NBD
637 fluorescence and an increase of its emission intensity. If PS extraction occurred in the presence
638 of an LTP (*e.g.,* Osh6p), the probe dissociated from the liposomes, and its fluorescence was lower.
639 In the PI(4)P extraction assay, liposomes were doped with 2 mol% PI(4)P, and 250 nM NBD-PH$_{FAPP}$
640 was used. (**C**) FRET-based lipid transport assays. In the PS transport assay, PC/PS/Rhod-PE
641 liposomes (93/5/2 mol/mol, L$_A$) were incubated with 250 nM NBD-C2$_{Lact}$. PC liposomes, doped or
642 not with 5 mol% PI(4)P, and Osh6p were added at t = 1 min and t = 4 min, respectively. If PS
643 transport occurs, this elicits a dequenching of the NBD signal corresponding to the translocation
644 of NBD-C2$_{Lact}$ from L$_A$ to L$_B$ liposomes. In the PI(4)P transport assay, L$_B$ liposomes doped with 5
645 mol% PI(4)P were incubated with 250 nM NBD-PH$_{FAPP}$. PC liposomes (L$_A$) doped or not with 5
646 mol% PS were added. If PI(4)P transport occurs, this causes a quenching of the NBD signal due to
647 the translocation of NBD-PH$_{FAPP}$ from L$_B$ to L$_A$ liposomes. Abbreviations: NBD = 7-nitrobenz-2-oxa-
648 1,3-diazol) fluorophore; NMR = nuclear magnetic resonance; FAPP1 = four-phosphate-adaptor
649 protein 1; PDB = Protein Data Bank; PS= phosphatidylserine; PC = phosphatidylcholine; LTP = lipid
650 transfer protein; Osh6p = oxysterol-binding protein (OSBP) homolog 6 protein; PI(4)P =
651 phosphatidylinositol 4-phosphate; FRET = fluorescence resonance energy transfer; Rhod-PE =
652 rhodamine-phycoerythrin; L$_A$ liposomes = liposomes composed of PC and doped with 5 mol% PS
653 and 2 mol% of Rhod-PE; L$_B$ liposomes = liposomes incorporating 5 mol% PI(4)P.
654

655 **Figure 2**: **NBD-C2$_{Lact}$ purification.** (**A**) SDS-PAGE analysis was used to check the presence of the
656 protein at different steps of the purification procedure before labeling. The arrowheads indicate
657 the position of the C2$_{Lact}$ domain (red arrowhead), of the GST alone (grey arrowhead), and of the
658 GST-C2$_{Lact}$ construct (black arrowhead). (**B**) UV-visible absorbance spectrum of NBD-C2$_{Lact}$. (**C**)
659 SDS-PAGE analysis of the purified NBD-C2$_{Lact}$. The first image was acquired under UV illumination
660 without staining and reveals the presence of the NBD-C2$_{Lact}$ construct as it emits fluorescence.
661 The second image shows the same gel after a protein staining procedure (see the **Table of**
662 **Materials**). Abbreviations: NBD = 7-nitrobenz-2-oxa-1,3-diazol) fluorophore; NBD-C2$_{Lact}$ = *N,N'*-
663 dimethyl-*N*-(thioacetyl)-*N'*-(7-nitrobenz-2-oxa-1,3-diazol-4-yl)ethylenediamine moiety linked to
664 the thiol function of C352 (NBD-C2$_{Lact}$) C2 domain of bovine lactadherin (PDB ID: 3BN6[48]); PDB =
665 Protein Data Bank; SDS-PAGE = sodium dodecylsulfate polyacrylamide gel electrophoresis; GST =
666 glutathione S-transferase; MW = molecular-weight size marker; UV = ultraviolet.
667

668 **Figure 3: Extraction assays.** (**A**) Fluorescence spectra of NBD-C2$_{Lact}$ (250 nM) measured upon

excitation at 460 nm in the presence of liposomes (80 μM, 2 mol% PS) in the absence or presence of 3 μM Osh6p. Reference spectra were recorded with pure PC liposomes incubated or not with NBD-C2$_{Lact}$ (left panel). Several spectra were recorded from different series of wells, corrected by subtracting the background scattering signal from DOPC liposomes alone and averaged (n=4, ± SEM). The percentage of accessible PS that was extracted is indicated (right panel). (**B**) Fluorescence spectra of NBD-PH$_{FAPP}$ (250 nM) mixed with liposomes (80 μM, 2 mol% PI(4)P) in the absence or presence of 3 μM Osh6p. Reference spectra recorded with PC liposomes in the presence and absence of the sensor are shown (left panel). Several spectra were recorded from different series of wells, corrected by subtracting the background scattering signal from DOPC liposomes alone and averaged (n=4, ± SEM). The percentage of accessible PI(4)P that was extracted is indicated (right panel). Abbreviations: NBD = 7-nitrobenz-2-oxa-1,3-diazol) fluorophore; NBD-C2$_{Lact}$ = *N,N'*-dimethyl-*N*-(thioacetyl)-*N'*-(7-nitrobenz-2-oxa-1,3-diazol-4-yl)ethylenediamine moiety linked to the thiol function of C352 (NBD-C2$_{Lact}$) C2 domain of bovine lactadherin (PDB ID: 3BN6[48]); PDB = Protein Data Bank; PS= phosphatidylserine; PC = phosphatidylcholine; DOPC = dioleoylphosphatidylcholine; Osh6p = oxysterol-binding protein (OSBP) homolog 6 protein; PI(4)P = phosphatidylinositol 4-phosphate; SEM = standard error of the mean; a.u. = arbitrary units.

Figure 4: Typical PS transport kinetics measured with Osh6p and reference curve. (**A**) L$_B$ liposomes devoid of PI(4)P (200 μM total lipids) and Osh6p (200 nM) were sequentially added to a cuvette containing NBD-C2$_{Lact}$ (250 nM) and L$_A$ liposomes (200 μM) doped with 5 mol% PS and 2 mol% Rhod-PE (left curve). The same experiment was performed with L$_B$ liposomes doped with 5 mol% PI(4)P (middle curve). To determine F$_{Eq}$, NBD-C2$_{Lact}$ (250 nM) was premixed with L$_{A-Eq}$ liposomes; then, L$_{B-Eq}$ liposomes were added (right curve). (**B**) Averaged PS transport curves determined after the normalization of several measurements done using L$_B$ liposomes with or without PI(4)P (mean ± SEM, n=3). (**E**) Initial PS transfer rates (mean ± SEM, n=3). Abbreviations: NBD = 7-nitrobenz-2-oxa-1,3-diazol) fluorophore; NBD-C2$_{Lact}$ = *N,N'*-dimethyl-*N*-(thioacetyl)-*N'*-(7-nitrobenz-2-oxa-1,3-diazol-4-yl)ethylenediamine moiety linked to the thiol function of C352 (NBD-C2$_{Lact}$) C2 domain of bovine lactadherin (PDB ID: 3BN6[48]); PDB = Protein Data Bank; PS= phosphatidylserine; Osh6p = oxysterol-binding protein (OSBP) homolog 6 protein; PI(4)P = phosphatidylinositol 4-phosphate; Rhod-PE = rhodamine-phycoerythrin; L$_A$ liposomes = liposomes composed of phosphatidylcholine and doped with 5 mol% PS and 2 mol% of Rhod-PE; L$_B$ liposomes = liposomes incorporating 5 mol% PI(4)P; F = fluorescence; F$_0$ = fluorescence corresponding to NBD before addition of Osh6p; F$_{Eq}$ = fluorescence signal if PS fully equilibrated between L$_A$ and L$_B$ liposomes by a transfer process; SEM = standard error of the mean.

Figure 5: Typical PI(4)P transport kinetics measured with Osh6p and reference curve. (**A**) PS-free liposomes containing 2 mol% Rhod-PE (L$_A$, 200 μM total lipids) and Osh6p (200 nM) were sequentially added to a cuvette containing NBD-PH$_{FAPP}$ (250 nM) and L$_B$ liposomes (200 μM) doped with 5 mol% PI(4)P (left curve). The same experiment was performed with L$_A$ liposomes doped with 5 mol% PS (middle curve). To determine F$_{Eq}$, NBD-PH$_{FAPP}$ (250 nM) was premixed with L$_{B-Eq}$ liposomes; then, L$_{A-Eq}$ liposomes were added (right curve). (**B**) PI(4)P transfer kinetics determined after normalization of several measurements of L$_A$ liposomes with or without PS (mean ± SEM, n=3). (**C**) Initial PI(4)P transfer rates (mean ± SEM, n=3). Abbreviations: NBD = 7-

713 nitrobenz-2-oxa-1,3-diazol) fluorophore; NBD-PH$_{FAPP}$ = NBD-labeled Pleckstrin homology domain
714 of the human PI(4)P adapter protein, four-phosphate-adaptor protein 1 (FAPP1, UniProt:
715 Q9HB20, segment [1-100]); PS= phosphatidylserine; Osh6p = oxysterol-binding protein (OSBP)
716 homolog 6 protein; PI(4)P = phosphatidylinositol 4-phosphate; Rhod-PE = rhodamine-
717 phycoerythrin; L$_A$ liposomes = liposomes composed of phosphatidylcholine and doped with 5
718 mol% PS and 2 mol% of Rhod-PE; L$_B$ liposomes = liposomes incorporating 5 mol% PI(4)P; F =
719 fluorescence; F$_0$ = fluorescence corresponding to NBD before addition of Osh6p; F$_{Eq}$ =
720 fluorescence signal if PS fully equilibrated between L$_A$ and L$_B$ liposomes by a transfer process;
721 SEM = standard error of the mean.
722
723 **Table 1: Volumes of lipid stock solutions to be mixed for liposome preparation.** Abbreviations:
724 PS= phosphatidylserine; PC = phosphatidylcholine; PI(4)P = phosphatidylinositol 4-phosphate;
725 Rhod-PE = rhodamine-phycoerythrin; DOPC = dioleoylphosphatidylcholine; 1-palmitoyl-2-oleoyl-
726 sn-glycero-3-phospho-L-serine; 16:0 Liss Rhod-PE = 1,2-dipalmitoyl-sn-glycero-3-
727 phosphoethanolamine-N-(lissamine rhodamine B sulfonyl) (ammonium salt).
728
729 **DISCUSSION:**
730 The outcomes of these assays directly rely on the signals of the fluorescent lipid sensors. Thus,
731 the purification of these probes labelled at a 1:1 ratio with NBD and without free NBD
732 fluorophore contamination is a critical step in this protocol. It is also mandatory to check whether
733 the LTP under examination is properly folded and not aggregated. The amount of LTP tested in
734 the extraction assays must be equal to or higher than that of accessible PS or PI(4)P molecules to
735 properly measure whether this LTP efficiently extracts these lipids. Indeed, NBD-C2$_{Lact}$ and NBD-
736 PH$_{FAPP}$ bind to PS and PI(4)P, respectively, following a classical saturation binding curve. Given
737 their respective affinities for PS and PI(4)P, these probes remain largely bound to the liposomes
738 even if the liposomes contain residual traces of these ligands. This can lead to the erroneous
739 conclusion that an LTP does not efficiently extract these lipids. The protocol relies on standard
740 and commercially available PC, PS, and PI(4)P subspecies that are 18:1/18:1-PC, 16:0/18:1-PS,
741 and 16:0/16:0-PI(4)P, respectively. Performing experiments using lipid species with other acyl
742 chains can give different results, as previously reported[12,35].
743
744 In the transfer assays, if the bulk lipid composition (not considering PS or PI(4)P) of L$_A$ and L$_B$
745 liposomes has to be modified, it is key to also perform the control experiments using L$_{A-Eq}$ and L$_{B-}$
746 $_{Eq}$ liposomes with a bulk composition similar to that of L$_A$ and L$_B$ liposomes, respectively. The same
747 principle applies for the extraction assays. Genetically encoded fluorescent lipid-binding domains
748 are broadly used to analyze lipid distribution inside cells[44]. Caution is recommended when
749 analyzing such experiments as the association of these lipid probes with the membrane, although
750 primarily driven by the presence of the targeted lipid, can be influenced by other parameters
751 (density of anionic lipids, lipid-packing) that differ between cell compartments. In these assays,
752 the composition of liposomes is much simpler than that of cellular membranes: they are mostly
753 made of PC, a zwitterionic lipid, and thereby expose a rather inert surface that does not impact
754 how PS and PI(4)P are recognized by their corresponding sensor. PH$_{FAPP}$ can be used in the
755 presence of anionic lipids, such as PS, phosphatidic acid (PA), and PI[32], and C2$_{Lact}$ does not
756 recognize PI(4)P[12]; both these observations allow unbiased measurements of PS/PI(4)P

757   exchange. NBD-PH$_{FAPP}$ is not influenced by sterol[43].

758

759   However, it is not known whether these probes, in particular, NBD-C2$_{Lact}$, can be used with
760   liposomes with extreme features (*e.g.,* very low or high lipid-packing, highly negatively charged
761   surface, presence of lipid domains). Despite this potential limitation with respect to liposome
762   composition, this method based on fluorescent sensors has tremendous advantages compared
763   to other methods. First, it does not rely on fluorescently labeled PS and PI(4)P that bear an extra
764   bulky group and are likely not properly accommodated by the binding pocket of LTPs. Second,
765   these transport assays offer far better time resolution than methods based on liposome
766   separation (radioactivity-based assays[45] or mass spectrometry[33]), and it should be noted that
767   radiolabeled PI(4)P and PS are not commercially available. The capacity of a protein to transfer
768   PS or PI(4)P is not impacted by the association of the fluorescent sensors with liposomes. Indeed,
769   if the amount of NBD-C2$_{Lact}$ or NBD-PH$_{FAPP}$ and that of PS and PI(4)P in the outer leaflet of
770   liposomes that is accessible to the LTP is considered, only 5% of PS or PI(4)P are associated with
771   probe during a kinetics measurement.

772

773   Moreover, only 0.55–0.86% of the membrane surface is covered by the probe, considering the
774   total surface of liposomes (L$_A$+L$_B$ liposomes; 5.1×10^{16} nm^2 with an area of 0.7 nm^2 per lipid)—
775   the membrane surface that one individual C2 or PH molecule can occupy ($\approx$3.1 and 4.8 nm^2,
776   respectively, estimated from references[46-48]) and their concentration (250 nM). Thus, the
777   principles underlying these assays are adapted to properly analyze the kinetic and mechanistic
778   aspects of LTPs. As mentioned in the introduction, alterations in the activity of ORP5/8 can lead
779   to cellular dysfunctions[49]. For example, the invasiveness of pancreatic cancer cells seems to rely
780   on the level of ORP5 expression. Moreover, a causality exists between high levels of ORP5
781   expression and the poor prognosis of human pancreatic cancer. A high level of ORP5 expression
782   is also detected in lung tumor tissues, and more particularly, in metastatic cases. Interestingly,
783   the ability of ORP5 to transfer lipids might explain why it promotes cell proliferation and
784   migration.

785

786   ORP5 upregulates the mammalian target of rapamycin complex 1 (mTORC1) complex, which
787   plays a central role in cell survival and proliferation, probably because it enhances the activity of
788   Akt, an upstream activator of mTORC1, by supplying the PM with PS. Overall, these observations
789   suggest that ORP5 might be an interesting pharmacological target, and that these *in vitro* assays
790   might serve to screen molecules that are able to inhibit its activity. This assay can also help to
791   better define whether other members of the ORP/Osh family are PS/PI(4)P exchangers. Notably,
792   ORP10 was found to encapsulate PS *in vitro* and transfer PS in ER-Golgi contact sites[27,50], but it is
793   still unknown whether it acts as a PS/PI(4)P exchanger. Furthermore, these protocols can serve
794   to explore the ability of LTPs belonging to other families to transport PI(4)P, as was recently
795   shown with steroidogenic acute regulatory transfer-like proteins[10], or PS. Additionally, NBD-
796   PH$_{FAPP}$ has been used to follow the ability of LTP to transport PI(4,5)P$_2$ between liposomes, as it
797   recognizes this PIP[10,35]. Finally, this strategy could be adapted to measure other extraction or
798   transport processes *in vitro* by using other lipid-binding domains (*e.g.,* a non-catalytic PI-PLC to
799   detect PI[51], sporulation-specific protein 20 fragment to detect PA[52], domain 4 (D4) of
800   perfringolysin O to detect sterol[53]).

806
DISCLOSURES:
The authors declare that there are no conflicts of interest.

809
REFERENCES
1   Drin, G. Topological regulation of lipid balance in cells. *Annual Review of Biochemistry.* **83**, 51–77 (2014).
2   Bigay, J., Antonny, B. Curvature, lipid packing, and electrostatics of membrane organelles: defining cellular territories in determining specificity. *Developmental Cell.* **23** (5), 886–895 (2012).
3   Prinz, W. A. Lipid trafficking sans vesicles: where, why, how? *Cell.* **143** (6), 870–874 (2010).
4   Holthuis, J. C., Menon, A. K. Lipid landscapes and pipelines in membrane homeostasis. *Nature.* **510** (7503), 48–57 (2014).
5   Wong, L. H., Copic, A., Levine, T. P. Advances on the transfer of lipids by lipid transfer proteins. *Trends in Biochemical Sciences.* **42** (7), 516–530 (2017).
6   Wong, L. H., Gatta, A. T., Levine, T. P. Lipid transfer proteins: the lipid commute via shuttles, bridges and tubes. *Nature Reviews Molecular Cell Biology.* **20** (2), 85–101 (2019).
7   Iaea, D. B., Dikiy, I., Kiburu, I., Eliezer, D., Maxfield, F. R. STARD4 membrane interactions and sterol binding. *Biochemistry.* **54** (30), 4623–4636 (2015).
8   Wilhelm, L. P. et al. STARD3 mediates endoplasmic reticulum-to-endosome cholesterol transport at membrane contact sites. *The EMBO Journal.* **36** (10), 1412–1433 (2017).
9   Bian, X., Saheki, Y., De Camilli, P. Ca(2+) releases E-Syt1 autoinhibition to couple ER-plasma membrane tethering with lipid transport. *The EMBO Journal.* **37** (2), 219–234 (2018).
10   Horenkamp, F. A., Valverde, D. P., Nunnari, J., Reinisch, K. M. Molecular basis for sterol transport by StART-like lipid transfer domains. *The EMBO Journal.* **37** (6), e98002 (2018).
11   Jentsch, J. A. et al. Structural basis of sterol binding and transport by a yeast StARkin domain. *The Journal of Biological Chemistry.* **293** (15), 5522–5531 (2018).
12   Moser von Filseck, J. et al. INTRACELLULAR TRANSPORT. Phosphatidylserine transport by ORP/Osh proteins is driven by phosphatidylinositol 4-phosphate. *Science.* **349** (6246), 432–436 (2015).
13   Daum, G. et al. Systematic analysis of yeast strains with possible defects in lipid metabolism. *Yeast.* **15** (7), 601–614 (1999).
14   Ejsing, C. S. et al. Global analysis of the yeast lipidome by quantitative shotgun mass spectrometry. *Proceedings of the National Academy of Sciences of the United States of America.* **106** (7), 2136–2141 (2009).
15   Leidl, K., Liebisch, G., Richter, D., Schmitz, G. Mass spectrometric analysis of lipid species of human circulating blood cells. *Biochimica et Biophysica Acta.* **1781** (10), 655–664 (2008).
16   Sampaio, J. L. et al. Membrane lipidome of an epithelial cell line. *Proceedings of the National Academy of Sciences of the United States of America.* **108** (5), 1903–1907 (2011).
17   Vance, J. E., Steenbergen, R. Metabolism and functions of phosphatidylserine. *Progress in*

845   *Lipid Research.* **44** (4), 207–234 (2005).

846   18   Zinser, E. et al. Phospholipid synthesis and lipid composition of subcellular membranes in
847   the unicellular eukaryote *Saccharomyces cerevisiae*. *Journal of Bacteriology.* **173** (6), 2026–2034
848   (1991).

849   19   Leventis, P. A., Grinstein, S. The distribution and function of phosphatidylserine in cellular
850   membranes. *Annual Review of Biophysics.* **39**, 407–427 (2010).

851   20   Yeung, T. et al. Membrane phosphatidylserine regulates surface charge and protein
852   localization. *Science.* **319** (5860), 210–213 (2008).

853   21   Kim, J., Shishido, T., Jiang, X., Aderem, A., McLaughlin, S. Phosphorylation, high ionic
854   strength, and calmodulin reverse the binding of MARCKS to phospholipid vesicles. *Journal of*
855   *Biological Chemistry.* **269** (45), 28214–28219 (1994).

856   22   Sigal, C. T., Zhou, W., Buser, C. A., McLaughlin, S., Resh, M. D. Amino-terminal basic
857   residues of Src mediate membrane binding through electrostatic interaction with acidic
858   phospholipids. *Proceedings of the National Academy of Sciences.* **91** (25), 12253–12257 (1994).

859   23   Bivona, T. G. et al. PKC regulates a farnesyl-electrostatic switch on K-Ras that promotes
860   its association with Bcl-XL on mitochondria and induces apoptosis. *Molecular Cell.* **21** (4), 481–
861   493 (2006).

862   24   Finkielstein, C. V., Overduin, M., Capelluto, D. G. Cell migration and signaling specificity is
863   determined by the phosphatidylserine recognition motif of Rac1. *The Journal of Biological*
864   *Chemistry.* **281** (37), 27317–27326 (2006).

865   25   Bolsover, S. R., Gomez-Fernandez, J. C., Corbalan-Garcia, S. Role of the
866   Ca2+/Phosphatidylserine Binding Region of the C2 Domain in the Translocation of Protein Kinase
867   Cα to the Plasma Membrane. *Journal of Biological Chemistry.* **278** (12), 10282–10290 (2003).

868   26   Vance, J. E., Tasseva, G. Formation and function of phosphatidylserine and
869   phosphatidylethanolamine in mammalian cells. *Biochimica et Biophysica Acta.* **1831** (3), 543–554
870   (2013).

871   27   Maeda, K. et al. Interactome map uncovers phosphatidylserine transport by oxysterol-
872   binding proteins. *Nature.* **501** (7466), 257–261 (2013).

873   28   D'Ambrosio, J. M. et al. Osh6 requires Ist2 for localization to ER-PM contacts and efficient
874   phosphatidylserine transport in budding yeast. *Journal of Cell Science.* **133** (11), jcs243733 (2020).

875   29   Manford, A. G., Stefan, C. J., Yuan, H. L., Macgurn, J. A., Emr, S. D. ER-to-plasma membrane
876   tethering proteins regulate cell signaling and ER morphology. *Developmental Cell.* **23** (6), 1129–
877   1140 (2012).

878   30   Collado, J. et al. Tricalbin-mediated contact sites control ER curvature to maintain plasma
879   membrane integrity. *Developmental Cell.* **51** (4), 476–487 e477 (2019).

880   31   Hoffmann, P. C. et al. Tricalbins contribute to cellular lipid flux and form curved ER-PM
881   contacts that are bridged by rod-shaped structures. *Developmental Cell.* **51** (4), 488–502 e488
882   (2019).

883   32   Lipp, N. F. et al. An electrostatic switching mechanism to control the lipid transfer activity
884   of Osh6p. *Nature Communications.* **10** (1), 3926 (2019).

885   33   Chung, J. et al. INTRACELLULAR TRANSPORT. PI4P/phosphatidylserine countertransport
886   at ORP5- and ORP8-mediated ER-plasma membrane contacts. *Science.* **349** (6246), 428–432
887   (2015).

888   34   Sohn, M. et al. PI(4,5)P2 controls plasma membrane PI4P and PS levels via ORP5/8

889 recruitment to ER-PM contact sites. *The Journal of Cell Biology.* **217** (5), 1797–1813 (2018).

890 35 Ghai, R. et al. ORP5 and ORP8 bind phosphatidylinositol-4, 5-biphosphate (PtdIns(4,5)P 2)
891 and regulate its level at the plasma membrane. *Nature Communications.* **8** (1), 757 (2017).

892 36 Sohn, M. et al. Lenz-Majewski mutations in PTDSS1 affect phosphatidylinositol 4-
893 phosphate metabolism at ER-PM and ER-Golgi junctions. *Proceedings of the National Academy*
894 *of Sciences of the United States of America.* **113** (16), 4314–4319 (2016).

895 37 Kattan, W. E. et al. Targeting plasma membrane phosphatidylserine content to inhibit
896 oncogenic KRAS function. *Life Science Alliance.* **2** (5), e201900431 (2019).

897 38 Du, X., Turner, N., Yang, H. The role of oxysterol-binding protein and its related proteins
898 in cancer. *Seminars in Cell & Developmental Biology.* **81**, 149–153 (2018).

899 39 Galmes, R. et al. ORP5/ORP8 localize to endoplasmic reticulum-mitochondria contacts
900 and are involved in mitochondrial function. *EMBO reports.* **17** (6), 800–810 (2016).

901 40 Du, X. et al. ORP5 localizes to ER-lipid droplet contacts and regulates the level of PI(4)P on
902 lipid droplets. *The Journal of Cell Biology.* **219** (1), e201905162 (2020).

903 41 Wang, H. et al. ORP2 delivers cholesterol to the plasma membrane in exchange for
904 phosphatidylinositol 4, 5-bisphosphate (PI(4,5)P2). *Molecular Cell.* **73** (3), 458–473 e457 (2019).

905 42 Kay, J. G., Grinstein, S. Sensing phosphatidylserine in cellular membranes. *Sensors (Basel).*
906 **11** (2), 1744–1755 (2011).

907 43 Moser von Filseck, J., Vanni, S., Mesmin, B., Antonny, B., Drin, G. A phosphatidylinositol-
908 4-phosphate powered exchange mechanism to create a lipid gradient between membranes.
909 *Nature Communications.* **6**, 6671 (2015).

910 44 Wills, R. C., Goulden, B. D., Hammond, G. R. V. Genetically encoded lipid biosensors.
911 *Molecular Biology of the Cell.* **29** (13), 1526–1532 (2018).

912 45 Raychaudhuri, S., Im, Y. J., Hurley, J. H., Prinz, W. A. Nonvesicular sterol movement from
913 plasma membrane to ER requires oxysterol-binding protein-related proteins and
914 phosphoinositides. *The Journal of Cell Biology.* **173** (1), 107–119 (2006).

915 46 Lenoir, M. et al. Structural basis of wedging the Golgi membrane by FAPP pleckstrin
916 homology domains. *EMBO reports.* **11** (4), 279–284 (2010).

917 47 Liu, Y., Kahn, R. A., Prestegard, J. H. Interaction of Fapp1 with Arf1 and PI4P at a
918 membrane surface: an example of coincidence detection. *Structure.* **22** (3), 421–430 (2014).

919 48 Shao, C., Novakovic, V. A., Head, J. F., Seaton, B. A., Gilbert, G. E. Crystal structure of
920 lactadherin C2 domain at 1.7A resolution with mutational and computational analyses of its
921 membrane-binding motif. *The Journal of Biological Chemistry.* **283** (11), 7230–7241 (2008).

922 49 Lipp, N. F., Ikhlef, S., Milanini, J., Drin, G. Lipid exchangers: cellular functions and
923 mechanistic links with phosphoinositide metabolism. *Frontiers in Cell and Developmental*
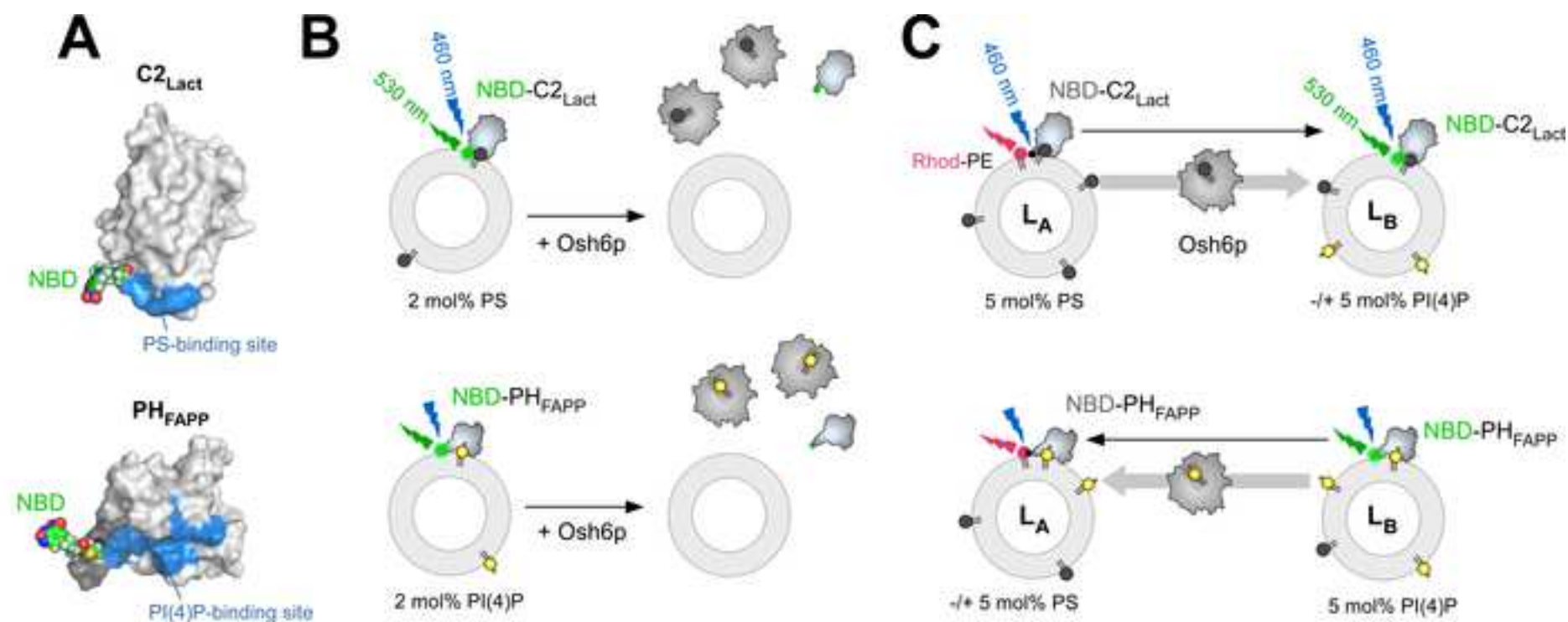924 *Biology.* **8**, 663 (2020).

925 50 Venditti, R. et al. Molecular determinants of ER-Golgi contacts identified through a new
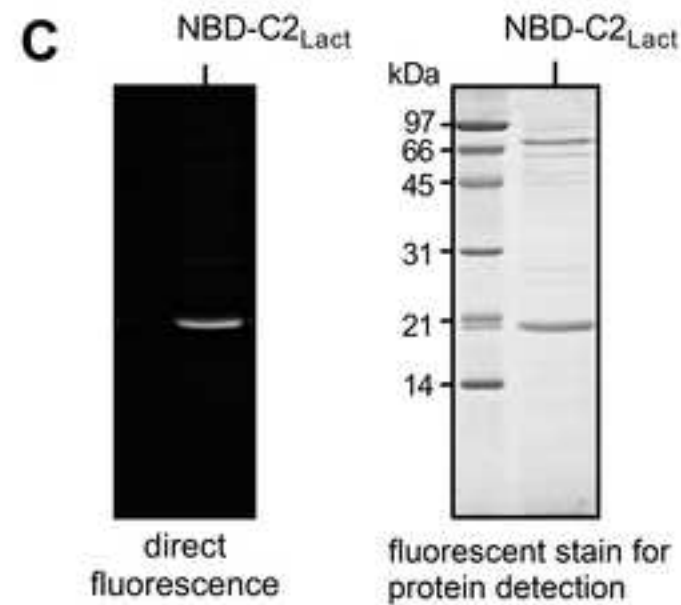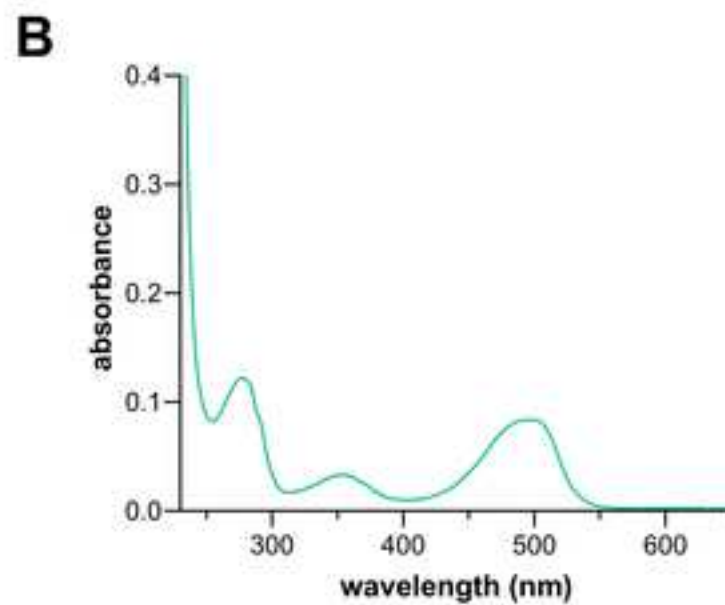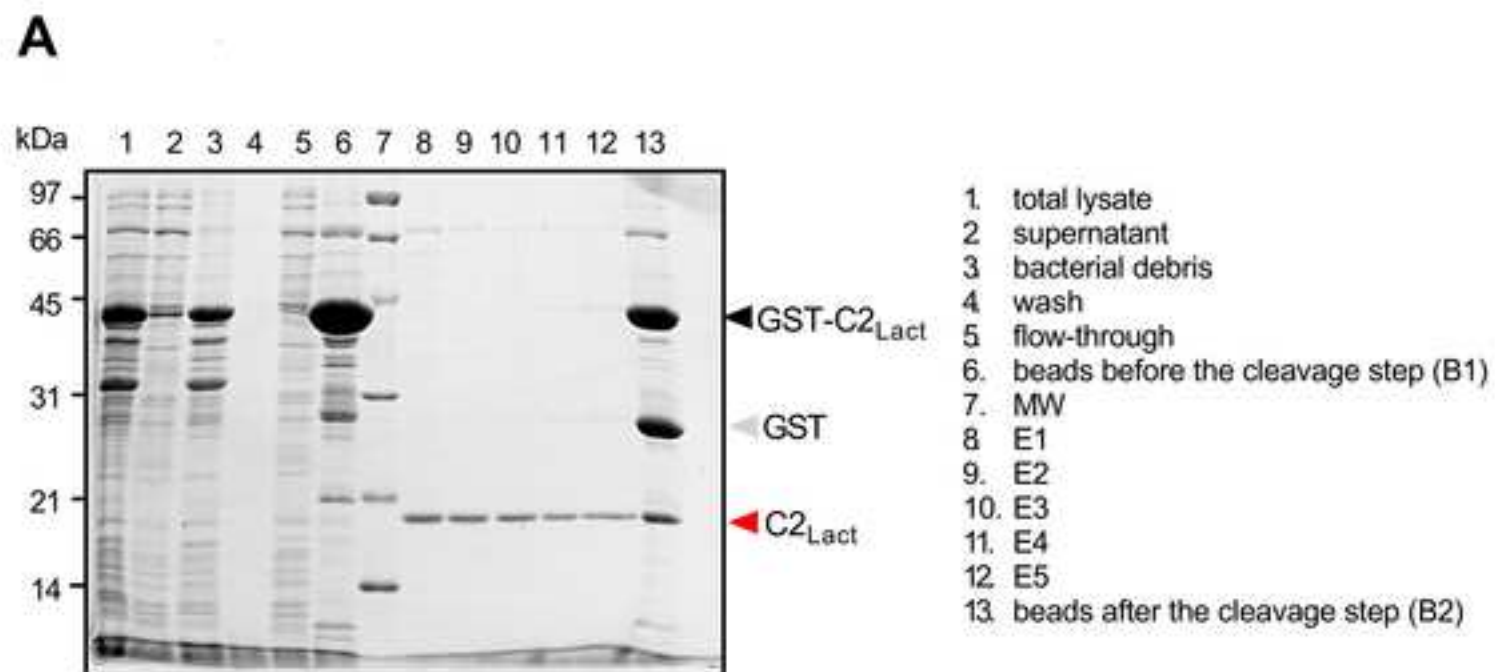926 FRET-FLIM system. *The Journal of Cell Biology.* **218** (3), 1055–1065 (2019).

927 51 Pemberton, J. G. et al. Defining the subcellular distribution and metabolic channeling of
928 phosphatidylinositol. *The Journal of Cell Biology.* **219** (3), doi: 10.1083/jcb.201906130 (2020).
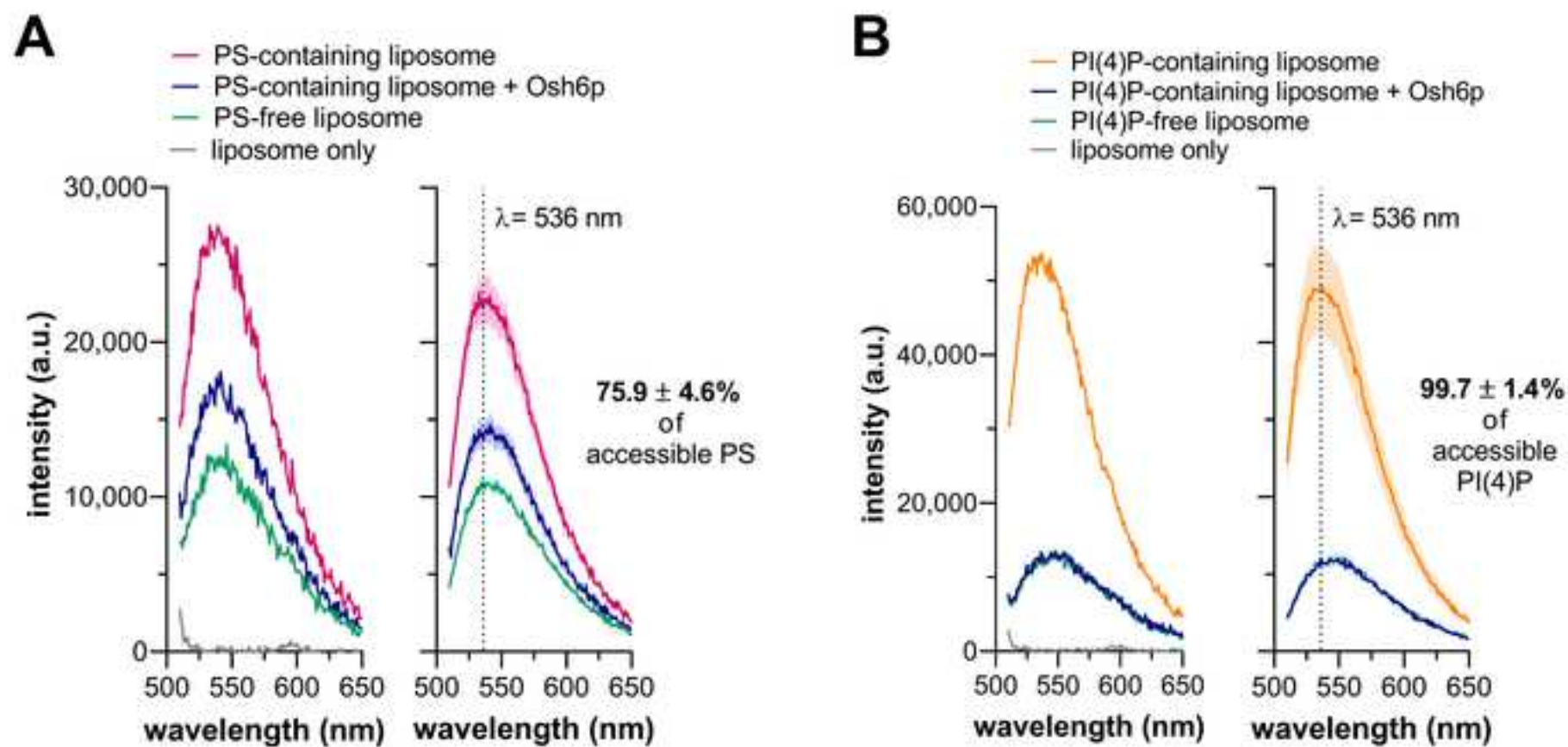
929 52 Nakanishi, H., de los Santos, P. & Neiman, A. M. Positive and negative regulation of a
930 SNARE protein by control of intracellular localization. *Molecular Biology of the Cell.* **15** (4), 1802–
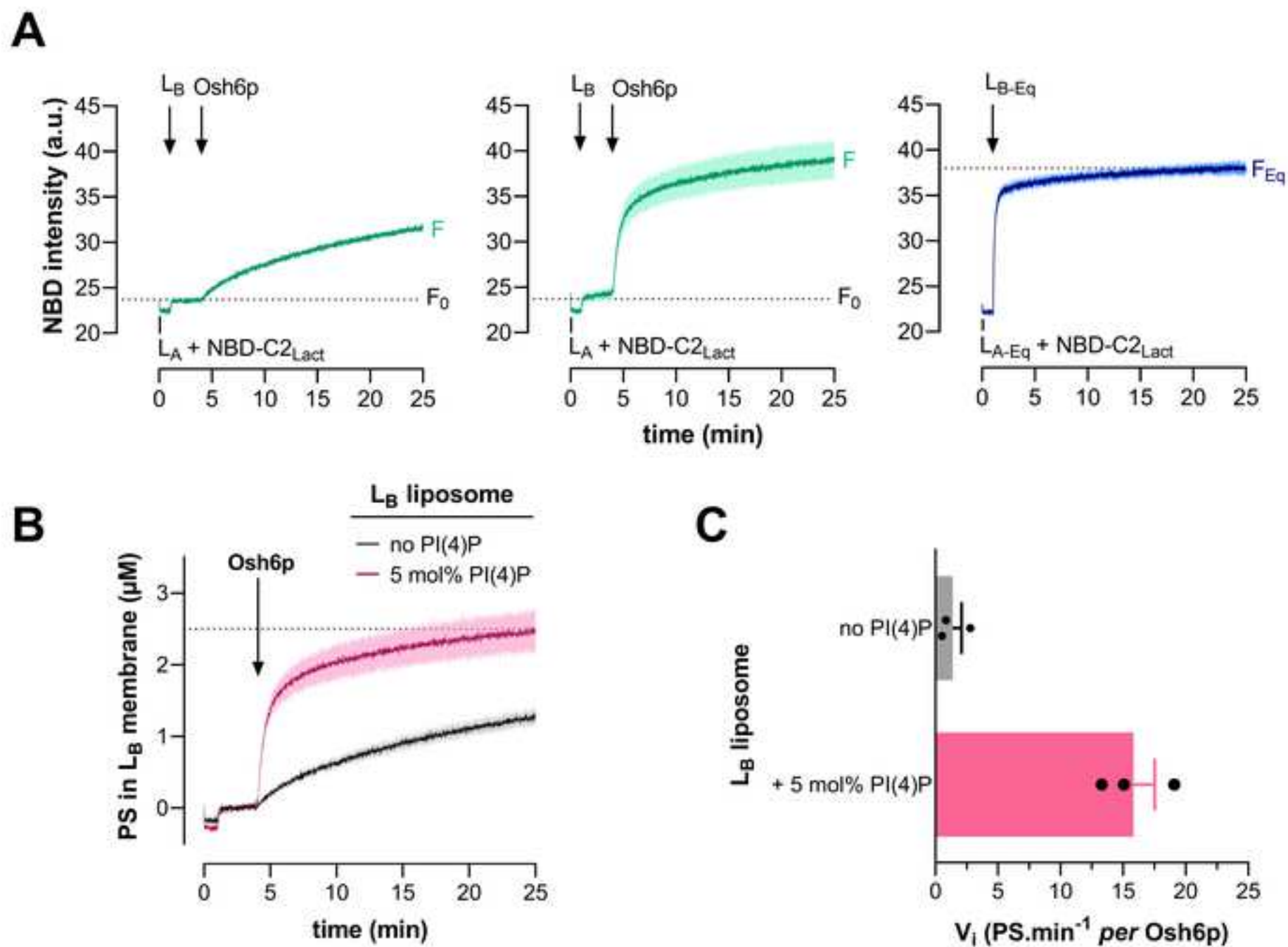931 1815 (2004).

932 53 Maekawa, M., Yang, Y., Fairn, G. D. Perfringolysin O theta toxin as a tool to monitor the

933   distribution and inhomogeneity of cholesterol in cellular membranes. *Toxins.* **8** (3), 67 (2016).
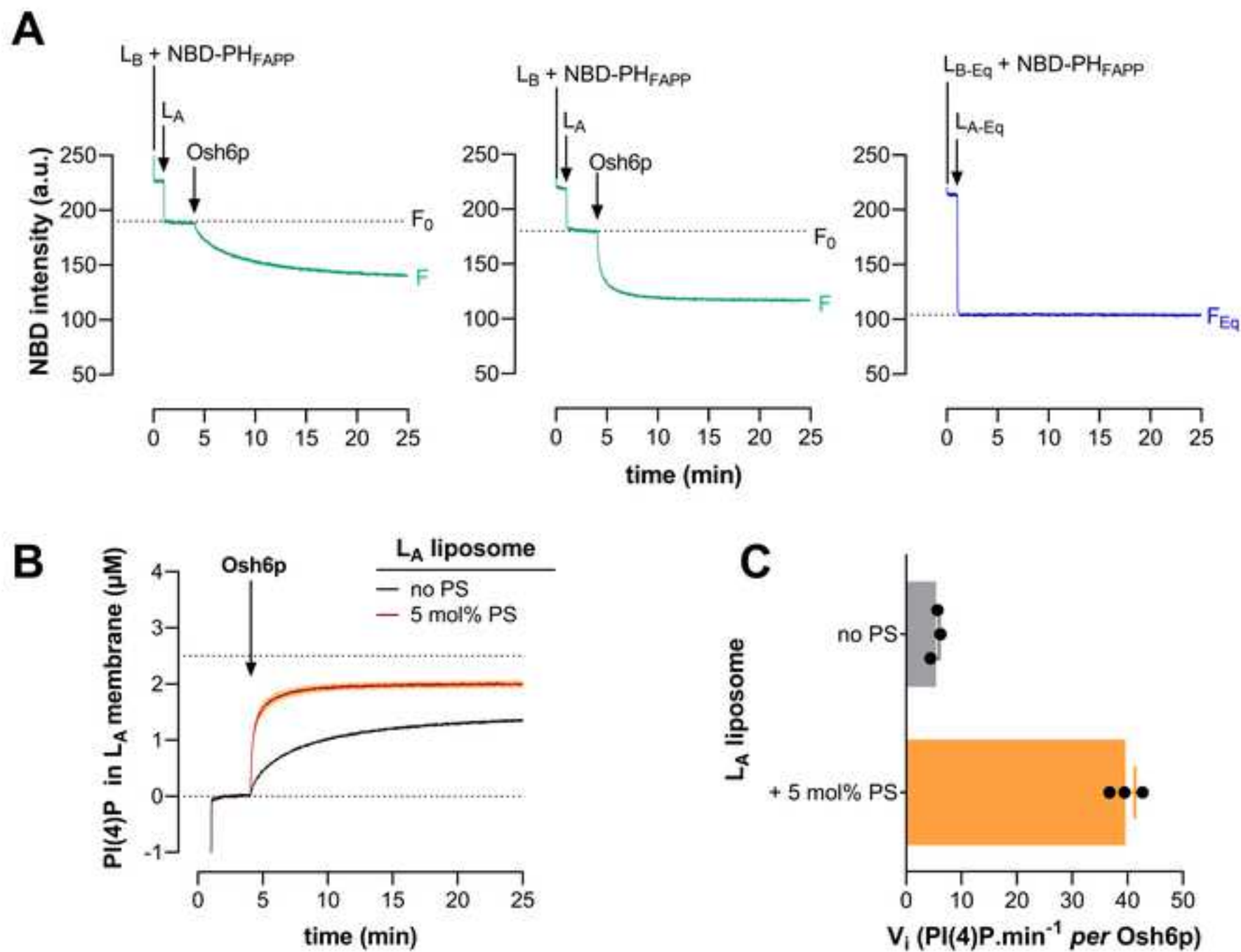934
935

Figure 1

Figure 2   Click here to access/download;Figure;Fig2-JOVE-revised.jpg ⬇

A

kDa   1 2 3 4 5 6 7 8 9 10 11 12 13

GST-C2Lact
GST
C2Lact

1. total lysate
2. supernatant
3. bacterial debris
4. wash
5. flow-through
6. beads before the cleavage step (B1)
7. MW
8. E1
9. E2
10. E3
11. E4
12. E5
13. beads after the cleavage step (B2)

B

absorbance vs wavelength (nm)

C

NBD-C2Lact — direct fluorescence

NBD-C2Lact — fluorescent stain for protein detection

Figure 3   Click here to access/download;Figure;Fig3-JOVE-revised.jpg ⬇

Figure 4 Click here to access/download;Figure;Fig4-JOVE-revised.tif

Figure 5

Click here to access/download;Figure;Fig5-JOVE-revised.tif ⬇

Table 1. Volumes of lipid stock solutions to be mixed for liposome preparation

	Liposome name	Lipid composition (mol/mol)	DOPC (25 mg/mL)	POPS (10 mg/mL)	16:0 Liss Rhod-PE (1 mg/mL)	C16:0/C16:0-PI(4)P (1 mg/mL)
Extraction assays	Liposome 2 mol% PS	PC/PS 98/2	247 µL	12.5 µL		
	Liposome 2 mol% PI(4)P	PC/PI(4)P 98/2	247 µL			153 µL
	DOPC liposome	PC 100	252 µL			
Transport assays	L_A	PC/PS/Rhod-PE 93/5/2	234 µL	31.4 µL	200 µL	
	L_A without PS	PC/Rhod-PE 98/2	247 µL		200 µL	
	L_B	DOPC/PI(4)P 95/5	237 µL			383 µL
	L_B without PI(4)P	PC 100	252 µL			
	L_{A-Eq}	DOPC/PS/PI(4)P/Rhod-PE 93/2.5/2.5/2	234 µL	15.7 µL	200 µL	191 µL
	L_{B-Eq}	DOPC/PS/PI(4)P 95/2.5/2.5	239 µL	15.7 µL		191 µL

Name of Material/ Equipment	Company	Catalog Number	Comments/Description
L-cysteine ≥97 % (FG)	Sigma	W326305-100G	Prepare a 10 mM L-cysteine stock solution in water. Aliquots are stored at -20 °C
2 mL Amber Vial, PTFE/Rub Lnr, for lipids storage in $CHCL_3$	Wheaton	W224681	
4 mm-diameter glass beads	Sigma	Z265934-1EA	
50 mL conical centrifuge tube	Falcon		
ÄKTA purifier	GE healthcare		FPLC
Aluminium foil			
Amicon Ultra-15 with a MWCO of 3 and 10 kDa	Merck	UFC900324, UFC901024	
Amicon Ultra-4 with a MWCO of 3 and 10 kDa	Merck	UFC800324, UFC801024	
Ampicillin			Prepare a 50 mg/mL stock solution with filtered and sterilized water and store it at -20 °C.
Bestatin	Sigma	B8385-10mg	
BL21 Gold Competent Cells	Agilent		
C16:0 Liss (Rhod-PE) in $CHCl_3$ (1 mg/mL)	Avanti Polar Lipids	810158C-5MG	
C16:0/C16:0-PI(4)P	Echelon Lipids	P-4016-3	Dissolve 1 mg of C16:0/C16:0-PI(4)P powder in 250 µL of MeOH and 250 µL of $CHCl_3$. Then complete with $CHCl_3$ to 1 mL. The solution must become clear.
C16:0/C18:1-PS (POPS) in $CHCl_3$ (10 mg/mL)	Avanti Polar Lipids	840034C-25mg	
C18:1/C18:1-PC (DOPC) in $CHCl_3$ (25 mg/mL)	Avanti Polar Lipids	850375C-500mg	
$CaCl_2$	Sigma		Prepare 10 mM $CaCl_2$ stock solution in water.
Cell Disruptor	Constant Dynamics		
Chloroform ($CHCl_3$) RPE-ISO	Carlo Erba	438601	
Complete EDTA-free protease inhibitor cocktail	Roche	5056489001	
Deionized (Milli-Q) water			
Dimethylformamide (DMF), anhydrous, >99% pure			
DNAse I Recombinant, RNAse free, in powder	Roche	10104159001	
DTT	Euromedex	EU0006-B	Prepare 1 M DTT stock solution in Milli-Q water. Prepare 1 mL aliquots and store them at -20 °C.
Econo-Pac chromatography columns (1.5 × 12 cm).	Biorad	7321010	
Electroporation cuvette 2 mm	Ozyme	EP102	
Electroporator Eppendorf 2510	Eppendorf		
Fixed-Angle Rotor Ti45 and Ti45 tubes	Beckman		Spinning the batcerial lysates
Glass-syringes (10, 25, and 50 µL) for fluorescence experiment	Hamilton		
Glass-syringes (25 , 100, 250, 500, and 1000 µL) to handle lipid stock solutions	Hamilton	1702RNR, 1710RNR, 1725RNR, 1750RN type3, 1001RN	
Glutathione Sepharose 4B beads	GE Healthcare	17-0756-05	
Glycerol (99% pure)	Sigma	G5516-500ML	
Hemolysis tubes with a cap			
HEPES , >99 % pure	Sigma	H3375-500G	
Illustra NAP 10 desalting column	GE healthcare	GE17-0854-02	
Isopropyl β-D-1-thiogalactopyranoside (IPTG)	Euromedex	EU0008-B	Prepare 1 M IPTG stock solution in Milli-Qwater. Prepare 1 mL aliquots and store them at -20 °C.
K-Acetate	Prolabo	26664.293	
Lennox LB Broth medium without glucose			Prepared with milli-Q water and autoclaved.
Liquid nitrogen	Linde		
Methanol (MeOH) ≥99.8%	VWR	20847.24	
$MgCl_2$	Sigma		Prepare a 2 M $MgCl_2$ solution. Filter the solution using a 0.45 µm filter.
Microplate 96 Well PS F-Botom Black Non-Binding	Greiner Bio-one	655900	
Mini-Extruder with two 1 mL gas-tight Hamilton syringes	Avanti Polar Lipids	610023	
Monochromator-based fluorescence plate reader	TECAN	M1000 Pro	

Name	Supplier	Catalog #	Notes
N,N'-Dimethyl-N-(Iodoacetyl)-N'-(7-Nitrobenz-2-Oxa-1,3-Diazol-4-yl)Ethylenediamine) (IANBD Amide)	Molecular Probes		Dissolve 25 mg of IANBD in 2.5 mL of dimethylsulfoxide (DMSO) and prepare 25 aliquot of 100 µL in 1.5 mL screw-cap tubes. Do not completely screw the cap. Then, remove DMSO in a freeze-dryer to obtain 1 mg of dry IANBD *per* tube. Tubes are closed and stored at -20 °C in the dark.
NaCl	Sigma	S3014-1KG	
PBS			137 mM NaCl, 2.7 mM KCl, 10 mM NaH_2PO_4, 1.8 mM KH_2PO_4, autoclaved and stored at 4 °C.
Pear-shaped glass flasks (25 mL, 14/23, Duran glass)	Duran Group		
Pepstatin	Sigma	p5318-25mg	
pGEX-C2$_{LACT}$ plasmid			Available on request from our lab
pGEX-PH$_{FAPP}$ plasmid			Available on request from our lab
Phenylmethylsulfonyl fluoride (PMSF) ≥98.5% (GC)	Sigma	P7626-25g	Prepare a 200 mM PMSF stock solution in isopropanol
Phosphoramidon	Sigma	R7385-10mg	
Polycarbonate filters (19 mm in diameter) with pore size of 0.2 µm	Avanti Polar Lipids	610006	
Poly-Prep chromatography column (with a 0-2 mL bed volume and a 10 mL reservoir)	Biorad	7311550	
Prefilters (10 mm in diameter).	Avanti Polar Lipids	610014	
PyMOL	http://pymol.org/		Construction of the 3D models of the proteins (Figure 1A)
Quartz cuvette for UV/visible fluorescence (minimum volume of 600 µL)	Hellma		
Quartz cuvettes	Hellma		
Refrigerated centrifuge Eppendorf 5427R	Eppendorf		
Rotary evaporator	Buchi	B-100	
Screw-cap microcentriguge tubes (1.5 mL)	Sarsted		
Small magnetic PFTE stirring bar (5 × 2 mm)			
Snap-cap microcentriguge tubes (0.5, 1, and 2 mL)	Eppendorf		
SYPRO orange			fluorescent stain to detect protein in SDS-PAGE gel
Thermomixer	Starlab		
THROMBIN, FROM HUMAN PLASMA	Sigma	10602400001	Dissolve 20 units in 1 mL of milli-Q water and prepare 25 µL aliquots in 0.5 mL Eppendorf tubes. Then freeze and store at -80 °C.
Tris, ultra pure	MP	819623	
Ultracentrifuge L90K	Beckman		
UV/Visible absorbance spectrophotometer	SAFAS		
UV/visible spectrofluorometer with a temperature-controlled cell holder and stirring device	Jasco or Shimadzu	Jasco FP-8300 or Shimadzu RF-5301PC	
Vacuum chamber			
Water bath	Julabo		
XK 16/70 column packed with Sephacryl S200HR	GE healthcare		

Guillaume Drin
CNRS, Institut de Pharmacologie Moléculaire et Cellulaire
660 route des lucioles, 06560 Valbonne, France

Manuscript 62177_R2

> JOVE,
> Dr. Nam Nguyen
> Manager of Review
>
> Dr. Benjamin Werth
> Editor

Valbonne, February 4, 2021

Dear editors,

Please find enclosed a second revised version of our manuscript entitled "Fluorescence-based measurements of phosphatidylserine/phosphatidylinositol 4-phosphate exchange between membranes". We are delighted to read that both reviewers consider the manuscript suitable for publication. We have addressed their respective points by making textual changes in red in the manuscript and by revising Figure 4 and 5 as detailed in the point-by-point response letter.

Other textual changes: We have corrected some typos in the manuscript, added a few details, and corrected some inversions of terms in the Protocol section and Figure captions both referring to experiments shown in Figure 4A and Figure 5A (right panel). We have also rewritten the step 3 and 4 of Section 1.3 to better explain a calculation method. All these corrections are in blue. We have also reformatted the References by spelling out the journal names according to JOVE guidelines. We have modified the Protocol section to remove the notes.

We hope that the revised version of our manuscript is now suitable for publication in *JOVE*.

Sincerely yours,

Guillaume Drin

Point-by-point response to reviewers
Reviewer #1:
Manuscript Summary:

This very well written and explain manuscript describes in detail a protocol for the use of PS and PI4P recognizing protein domains (C2 and PH domains respectively) that have been engineered to contain one surface accessible cysteine residue to which has been conjugated a fluorescent 7-nitrobenoxadiazole group. This is used to detect the presence of the protein when bound to phospholipid vesicle membranes that contain the appropriate lipid. When a lipid transfer protein is added either PS or PI4P is removed from the membrane and the change in signal from the NBD group monitored to show lipid removal from the donor vesicle. In a similarly deigned FRET assay, a rhodamine-PE is used as the quenching fluorophore for the NBD group, and time-resolved transfer assays can be recorded. This is a cleverly designed assay system that should be a of general use to investigators interested in lipid transfer process driven by PI4P gradients. The text instructions are quite detailed, but easy to read. I have only minor cosmetic suggestions and word substitutions.

We would like to thank the reviewer for these very nice comments on our manuscript.

Minor Concerns:
Line 57; Perhaps change "compose" to "comprise"
We think it is maybe better to change "compose" into "constitute".
Line 61; "repartition" works just as well as "partition"
Done.
Line 72; Maybe replace "encapsulates" with "binds"
Usually we prefer to use the verb "encapsulate" (or "trap" or "accommodate" instead of "bind" to clearly indicate that a LTP captures a lipid inside a pocket and is not a peripheral protein that only recognizes the polar head of a lipid. However, as we mention in the same paragraph what is the mode of binding between a LTP and its ligands, we agree that the verb" bind" is not ambiguous and can be used.

Line75; "We found that Osh6p and Osh7p can trap an alternative PI(4)P lipid ligand." Perhaps re-write to say "We found that Osh6p and Osh7p can trap PI(4)P as an alternative lipid ligand."
We agree. The sentence has been corrected
Line 85; "ligand" to "ligands"
Done.
Line 114; "We reengineered this domain to include a single solvent-exposed cysteine, labelled, with a NBD group, near the PI(4)P binding site." Perhaps change to: "We reengineered this domain to include a single solvent-exposed cysteine, which canbe labelled with a NBD group, near the PI(4)P binding site."
We agree, this is more precise. This correction has been made.
Line 120: "If PS is massively extracted by …" to "If PS is nearly completely extracted by…"
We agree. The correction has been done.
Line 153: "Many steps must be carried OUT on ice …"
The correction has been made.
Line 155: Omit "good".
Done.
Line 156: Omit second "sufficient"
Done.
Line 311: "Size-exclusion chromatography is performed on a Sephacryl S200HR column,.." Size? Grams of gel? Dimensions of column?
We agree. These details were completely necessary. We now indicate the dimensions of the column and the volume of resin packed in the column according to supplier's guidelines.
Line 320: "Laemmli SAMPLE buffer"

We agree.

A part of the manuscript was highlighted in yellow according to JOVE guidelines to mention that this is the one which must be converted into a script for the video.

Line 373 and 400: Change "bandwidth" to "slit width"
We prefer to keep the term" bandwidth" because this is the parameter that appears in the two software that pilot the fluorescence plate reader and the fluorimeter that are used for the experiments and will be shown in the video

References: Is the use of "et al." for when there are more than four authors?
We have formatted the references according to JOVE guidelines, using the provide EndNote style file

Ref 28 has now been published.
Absolutely correct. This is now corrected
Figure 1 was a bit blurry in my review copy.
Likely due to a loose conversion of the original Tiff file into a PDF file. We have increased the resolution of all the Figures.
Figure 4b: Lines in the legend do not seem to have the color of the lines in the graph
Figure 5b: Lines in the legend do not seem to have the color of the lines in the graph
GrapPad Prism automatically assigns the lines of the legend box with the color used to draw the curves. Maybe this change of color is due to a conversion problem. The legend lines are now thicker, also to respond to a Reviewer #2's comment. We now hope that the color correspondence between the lines of the legend box and the curves is easier to appreciate.
Page 35: Comments/Description It wasn't clear to me where these were mentioned in the text.
I also had several (apparently) blank pages with and a couple with vestigial text (p 38 and 40). I'm not certain what happened here.
Page 35-40 result from the conversion of a separated Excel file ,in which the different reagents used in our protocols are listed, and its merging with the manuscript file.

Reviewer #2:
Manuscript Summary:
The manuscript elegantly summarizes the protocol of in vitro PS/PI4P extraction as well as PS/PI4P counter transport between liposomes. The fluorescence probes that the authors developed are quite useful tools to monitor the PS/PI4P transport, and the similar strategy could be adapted to the other lipid molecules. The manuscript is written in a very clear manner and is useful for many readers, so it deserves to be published. I have very minor concerns to be addressed before publication.
We are grateful to Reviewer 2 for his/her very kind comments on our manuscript

Minor Concerns:
I was wondering how long we should incubate the sample when measuring the extraction of PS and PI4P? Do you measure the spectrum shown in Figure 3 right after adding the material? Or, do you measure several samples with different incubation times at the same time? I thought it would be more helpful to add this kind of information.
PS and PI(4)P extraction processes measured with Osh6p are extremely rapid and extraction is completed in less than 2 min. This is what we observed when we first devised this assay using a standard fluorimeter at that time (Moser et al., 2015). For the experiments with a fluorescence plate reader, as it takes a few minutes to load the different wells and for the plate to reach the thermal equilibrium once in the machine, the extraction is completed when the reading of the plate is launched. We now indicate in one sentence that after an incubation time of 5 minutes, the extraction is completed, at least in the case of Osh6p.

Are the spectra shown in right panels of Fig. 3 normalized by subtracting the liposome only signals?
This is entirely exact. We now indicate in the caption of Figure 3 that the spectra measured with each NBD-labelled probe are corrected by subtracting the background signal of liposomes alone.

Lines next to no PI4P or no PS, etc (Fig. 4B and 5B) are too thin and difficult for me to see the color. I thought it would be easier to read if they were a little bolder.
We have corrected the Figure 4 and 5 to increase the thickness of the lines in the legend box and to more clearly visualize the color of each of these lines.